UNIVERSIDADE D
COIMBRA

Inês Catarina Campos de Oliveira

PARTHENOLIDE: THERAPEUTIC POTENTIAL IN MULTIPLE MYELOMA RESISTANT TO PROTEASOME INHIBITORS

VOLUME 1

Dissertação no âmbito do Mestrado em Bioquímica orientada pela Professora Doutora Ana Cristina Gonçalves, pela Mestre Joana Jorge e Professora Doutora Maria Carmen Martins de Carvalho Alpoim (orientadora interna), apresentada ao Departamento de Ciências da Vida.

Julho de 2021

UNIVERSIDADE D
COIMBRA

Inês Catarina Campos de Oliveira

PARTHENOLIDE: THERAPEUTIC POTENTIAL IN MULTIPLE MYELOMA RESISTANT TO PROTEASOME INHIBITORS

VOLUME 1

Dissertação no âmbito do Mestrado em Bioquímica orientada pela Professora Doutora Ana Cristina Gonçalves, pela Mestre Joana Jorge e Professora Doutora Maria Carmen Martins de Carvalho Alpoim (orientadora interna), apresentada ao Departamento de Ciências da Vida.

Julho de 2021

Agradecimentos

Apesar de uma dissertação mestrado se tratar de um trabalho individual, não teria sido possível levar cabo este projeto sem a ajuda de inúmeras pessoas às quais gostaria de agradecer:

À Professora Doutora Ana Cristina Gonçalves, pela orientação, apoio e disponibilidade demonstradas ao longo do último ano, por todos os conselhos e sugestões dados, mas também pelo estímulo constante para fazer mais e melhor.

À Professora Doutora Ana Bela Sarmento Ribeiro, pela oportunidade de poder trabalhar e desenvolver este trabalho no Laboratório de Oncobiologia e Hematologia e por toda a confiança depositada em mim.

À Raquel Alves e à Joana Jorge sem a ajuda incansável das quais não teria sido possível a realização dos protocolos experimentais necessários ao desenvolvimento deste projeto. Agradeço também pelo apoio e por incentivarem sempre o meu pensamento critico.

À Beatriz Lapa e à Maria Inês Costa pela ajuda constante no laboratório, pela motivação e pela disponibilidade demonstrada.

À Diana, à Tânia e ao Miguel, colegas com quem partilhei o espaço de trabalho, que foram fonte de motivação, ajuda recíproca e companheirismo ao mesmo tempo que proporcionaram momentos de descontração imprescindíveis.

A todos os outros colegas de mestrado que completam esta etapa comigo, por terem tornado estes últimos dois anos uma boa experiência.

Por fim, mas não menos importante, um enorme agradecimento aqueles que me apoiam incondicionalmente:

Ao meu grupo de amigos, a quem devo para além de um agradecimento, um pedido de desculpas por ter estado mais ausente em prol da realização da tese. Ao Henrique, por todas as vezes que com ele desabafei, por todo o carinho, paciência e pela coragem que me transmitiu. Foram cruciais nesta fase da minha vida pois sempre estiveram disponíveis para ouvir as minhas preocupações sem julgar. Pela camaradagem e pelos momentos de convívio que também são necessários.

À minha família, em particular aos meus primos, tios e padrinhos, pelo amor e apoio incondicional e por acreditarem sempre em mim. À minha avó, pelo interesse persistente na minha vida académica embora ainda não entenda o que faço.

Aos meus pais, sem os quais não estaria aqui. Por sempre apoiarem as minhas escolhas, por permitirem que eu siga o meu caminho, e por fazerem das minhas vitorias as suas vitorias também. À minha mãe, que nunca duvida das minhas capacidades, por ser uma fonte de inspiração e por estar sempre lá para mim. Ao meu irmão, pelo amor incondicional, por todo o auxílio e por nunca deixar de me ouvir mesmo quando eu sou uma irmãzinha chata.

A todos, o meu muito obrigado!

Resumo

O mieloma múltiplo (MM) é uma neoplasia hematológica caracterizada pela expansão de plasmócitos clonais que produzem imunoglobulinas monoclonais e pela presença de um ou mais eventos definidores de mieloma, que consistem em características *CRAB* (hipercalcemia, insuficiência renal, anemia e Lesões Osteolíticas/bone lesions) e/ou um ou mais biomarcadores de malignidade (plasmócitos clonais ≥ 60%, razão entre cadeias leves livres séricas envolvidas/não envolvidas ≥ 100, e presença de pelo menos uma lesão focal em exames de ressonância magnética).

A ativação do fator nuclear-kB (NF-κB) é um evento muito comum em MM, sendo este fator uma das moléculas mais importantes envolvidas na resposta inflamatória, ligando a inflamação crónica ao cancro. O NF-κB é um complexo homo ou heterodimérico que se apresenta geralmente na forma de dímeros p65-p50. Os dímeros ligam-se a locais específicos do DNA dos seus genes-alvo, promovendo a sua transcrição.

Apesar de existirem inúmeras possibilidades terapêuticas para um doente com MM incluindo inibidores do proteassoma (PIs), como bortezomib (BTZ), carfilzomib (CFZ) e ixazomib (IXZ) e imunomoduladores que aumentam a esperança média de vida dos doentes, ao mesmo tempo que melhoram a sua qualidade de vida, a resistência a fármacos ainda é um grande obstáculo que precisa ser ultrapassado. Consequentemente, os medicamentos disponíveis deixam de ser uma opção para aqueles que desenvolvem resistência. Por esse motivo, novos agentes anticancerígenos, tal como o partenolide (PTL), um inibidor da ativação do NF-kB, poderá ser necessário para ultrapassar a resistência a fármacos. Além da sua atividade anti tumoral ser mediada pela inibição da via de sinalização do NF-κB, o PTL também reduz o nível celular de glutationa e induz a produção de espécies reativas de oxigénio, induzindo *stresse* oxidativo.

Nesse contexto, o principal objetivo do presente projeto é avaliar o papel do PTL em contornar a resistência do mieloma múltiplo aos inibidores do proteassoma BTZ, CFZ e IXZ.

Para o efeito, foram utilizadas linhas celulares de MM sensíveis (H929) e resistentes aos inibidores de proteossoma BTZ, CFZ e IXZ (H929-BTZ, H929-CFZ e H929-IXZ, respetivamente) foram incubadas na presença e na ausência de PTL, e procedeu-se ao ensaio metabólico com resazurina para verificar a atividade metabólica

celular. O tipo de morte celular induzida pela PTL foi analisado não só por citometria de fluxo (CF), utilizando a dupla coloração com anexina-V e 7-AAD, mas também por microscopia ótica, após a coloração segundo o protocolo May-Grünwald Giemsa. Para além disso, verificou-se o efeito do PTL no ciclo celular por CF, utilizando a solução de iodeto de propídio/RNase. Também se verificaram os níveis de peróxidos intracelulares utilizando a sonda $DCFH_2$-DA e o nível do $\Delta\psi_M$ por CF. Por último, o efeito da PTL na expressão génica foi avaliado por qPCR.

Este projeto comprovou que o PTL é capaz de reduzir a atividade metabólica das linhas celulares estudadas, dependendo do tempo de incubação, da concentração e da linha celular. De facto, a linha celular resistente H929-IXZ mostrou-se menos sensível à ação do parthenolide. Assim, às 72 horas os valores do IC_{50} foram de 2,40; 0,96; 2,37 e 7,32 μM para as linhas celulares H929, H929-BTZ, H929-CFZ e H929-IXZ, respetivamente. Para além disso, o PTL induziu um aumento significativo na percentagem de células apoptóticas em todas as linhas celulares (H929-BTZ mostrou um aumento de 12%, H929-CFZ mostrou um aumento de 19,75% e H929-IXZ mostrou um aumento de 20%). Além do mencionado, nas células tratadas com PTL disso observou-se um aumentou dos níveis intracelulares de peróxidos em 1,40 vezes, 1,12 vezes, 1,14 vezes e em 1,32 vezes nas linhas celulares H929, H929-BTZ, H929-CFZ e H929-IXZ respetivamente. Paralelamente, verificou-se um aumento do rácio M/A de JC-1 de cerca de 1,41 vezes, 1,82 vezes, 2,60 vezes e 4,67 vezes nas linhas celulares H929, H929-BTZ, H929-CFZ e H929-IXZ respetivamente, sugerindo que o PTL induz diminuição do potencial de membrana mitocondrial.

Concluindo, este estudo provou que o PTL é capaz de contornar a resistência aos PIs, podendo constituir uma nova abordagem terapêutica no MM resistente a estes fármacos.

Palavras-chave:

- Mieloma múltiplo
- Resistência a fármacos
- Inibidores de proteossoma
- Parthenolide

Abstract

Multiple myeloma (MM) is a hematologic neoplasm characterized by the expansion of clonal plasma cells that produce monoclonal immunoglobulins and by the presence of one or more myeloma-defining events, which consist of CRAB features (hypercalcemia, renal failure, anemia and bone lesions) and/or one or more malignancy biomarkers (clonal plasma cells ≥ 60%, ratio of serum free light chains involved/not involved ≥ 100, and the presence of at least one focal lesion on MRI scans).

Activation of nuclear factor-kB (NF-κB) is a very common event in MM, and this factor is one of the most important molecules involved in the inflammatory response, linking chronic inflammation to cancer. NF-κB is a homo- or heterodimeric complex that is generally in the form of p65-p50 dimers. Dimers bind to specific locations in the DNA of their target genes, promoting their transcription.

Choosing the right treatment for a MM patient is a complicated decision as there are several therapeutic possibilities. Some of the treatment options include proteasome inhibitors (PIs) such as bortezomib (BTZ), carfilzomib (CFZ) and ixazomib (IXZ). Although the chemotherapeutic drugs used to treat MM increase the average life expectancy of patients, while improving their quality of life, drug resistance is still a major obstacle that needs to be addressed. Consequently, available drugs can end up not being an option for those who develop resistance. For this reason, new anticancer agents, such as parthenolide (PTL), are needed to overcome drug resistance.

In this context, the main objective of this project is to evaluate the role of PTL in circumventing multiple myeloma resistance to BTZ, CFZ and IXZ proteasome inhibitors. This compound exerts its anti-tumor activity by inhibiting the NF-κB signaling pathway. PTL also reduces the cellular level of glutathione and induces the production of reactive oxygen species, inducing oxidative stress.

For this purpose, MM cell lines that are sensitive (H929) and resistant to the proteosome inhibitors BTZ, CFZ and IXZ (H929-BTZ, H929-CFZ and H929-IXZ, respectively) were incubated in the presence of PTL, and the metabolic assay using resazurin was proceeded to verify the cellular metabolic activity. The type of cell death induced by PTL was analyzed not only by flow cytometry (FC), using annexin-V (AV)/7-AAD double staining, but also by optical microscopy, after the staining according to the May-Grünwald Giemsa protocol. Furthermore, the effect of PTL on the cell cycle was verified by FC using the propidium iodide/RNase solution. The levels of intracellular

peroxides were also verified using the probe DCFH2-DA and the level of $\Delta\psi_M$ by FC. Finally, the effect of PTL on gene expression was assessed by qPCR.

This project proved that PTL is able to reduce the metabolic activity of the cell lines studied, according to the incubation time and concentration used. Furthermore, resistant cell lines were generally less susceptible to the action of parthenolide. In fact, at 72 hours the IC50 values were 1.98, 1.20, 1.73 and 4.56 μM for cell lines H929, H929-BTZ, H929-CFZ and H929-IXZ, respectively. Furthermore, cell death analysis showed that PTL caused a significant increase in the percentage of apoptotic cells in all cell lines (H929-BTZ showed an increase of 12%, H929-CFZ showed an increase of 19.75% e H929-IXZ showed an increase of 20%). Furthermore, it increased intracellular peroxide levels by 1.40-fold, 1.12-fold, 1.14-fold and 1.32-fold in cell lines H929, H929-BTZ, H929-CFZ and H929-IXZ respectively. In parallel, there was an increase in the M/A ratio of 1.41-fold, 1.82-fold, 2.60-fold and 4.67-fold in cell lines H929, H929-BTZ, H929-CFZ and H929-IXZ respectively.

In conclusion, this study proved that PTL is able to overcome resistance to PIs and may constitute a new therapeutic approach in MM resistant to these drugs.

Keywords:

- Multiple myeloma
- Drug resistance
- Proteosome inhibitors
- Parthenolide

Table of contents

Abbreviations

$\Delta_{\Psi M}$ - Mitochondrial membrane potential

7-AAD - 7-amino-actinomycin D

APRIL - A proliferation-inducing ligand

ASCT - Autologous stem cell transplantation

ATCC - American Type Culture Collection

AV - Annexin V

BAFF - B-cell activating factor

BAX - BCL-2-associated X protein

BM - Bone marrow

BTZ - Bortezomib

cDNA - Complementary deoxyribonucleic acid

CFZ - Carfilzomib

CLP - Common lymphoid precursor

CMP - Common myeloid progenitor

CP- Core particle

CSCs - Cancer stem cells

CT - Cycle threshold

DCF - 2',7'-dichlorofluorescein

$DCFH_2$ - 2',7'-dichlorodihydrofluorescein

$DCFH_2$-DA - 2',7'-dichlorodihydrofluorescein diacetate

DMAPT - Dimethylamino-parthenolide

DMSO - Dimethyl sulfoxide

DNA - Deoxyribonucleic acid

DNTPs - Deoxyribonucleotides

EBF - Early B-cell factor 1

ELP - Early lymphoid progenitors

ER - Endoplasmic reticulum

FBS - Fetal bovine serum

FC - Flow cytometry

FGFR3 - Fibroblast growth factor

H_2O_2 - Hydrogen peroxide

H929-BTZ - H929 cell line resistant to bortezomib

H929-CFZ - H929 cell line resistant to carfilzomib

H929-IXZ – H929 cell line resistant to ixazomib

HGF - Hepatocyte growth factor

HSC - Hematopoietic stem cell

HSP-70 - Heat shock protein-70

IC_{50} - Half maximal inhibitory concentration

ICAM-1 - Intercellular adhesion molecule-1

Ig - Immunoglobulin

IGF-1- Insulin-like growth factor-1

IgH - Immunoglobulin heavy chain

IKKs - IkB kinases

IL - Interleukin

IMiDs - Immunomodulatory drugs

IXZ - Ixazomib

JAK/STAT - Janus kinase/signal transducers and activators of transcription

JC-1 - 5, 5´, 6, 6´-tetrachloro-1, 1´, 3, 3´-tetraethylbenzimidazolcarbocyanine

JNK - c-Jun N-terminal kinases

LFA-1 - Lymphocyte function-associated antigen-1

LPS - Bacterial lipopolysaccharide

MAPK - Mitogen-activated protein kinase

MDR - Multidrug resistance

MGUS - Monoclonal gammopathy of undetermined significance

MIP-1α - Macrophage inflammatory protein 1 alpha

MM - Multiple myeloma

MMSET - Multiple myeloma SET

MoAbs - Monoclonal antibodies

MPPs - Multipotent progenitors

MUC-1 - Mucin-1 antigen

MYC/c-MYC – Myelocytomatosis oncogene

NF-κB - Nuclear factor-kB

NIK - NF-κB-inducing kinase

NOXA - NADPH oxidase activator

PAX5 - Paired box 5

PBS - Phosphate buffered saline

PC - Plasma cells

PCR - Polymerase chain reaction

PI - Proteasome inhibitors

PS - Phosphatidylserine

PTEN - Phosphatase and tensin homolog

PTL - Parthenolide

RNA - Ribonucleic acid

ROS - Reactive oxygen species

RP - Regulatory particle

SDC1 - Syndecan-1

SL - Sesquiterpene lactone

TB - Trypan Blue

TNF-α - Tumor necrosis factor α

VCAM-1 - Vascular cell adhesion molecule-1

VLA-4 - Very late antigen-4

Introduction

1. Hematopoietic System

A dynamic equilibrium exists in the blood, which represents one of the most regenerative systems in the human body, between cell growth, differentiation, and death. A common hematopoietic progenitor cell constantly replenishes and rebuilds the many blood cell populations[1,2]. These hematopoietic stem cells, that also have the ability to self-renew, become more restricted in their developmental potential as they reach the myeloid and lymphoid lineages, producing differentiated and functional blood cells. Myeloid blood cells include erythrocytes, thrombocytes, macrophages, neutrophils, eosinophils, and basophils while B, T, and natural killer cells are held in the lymphoid group (Figure 1)[3,4].

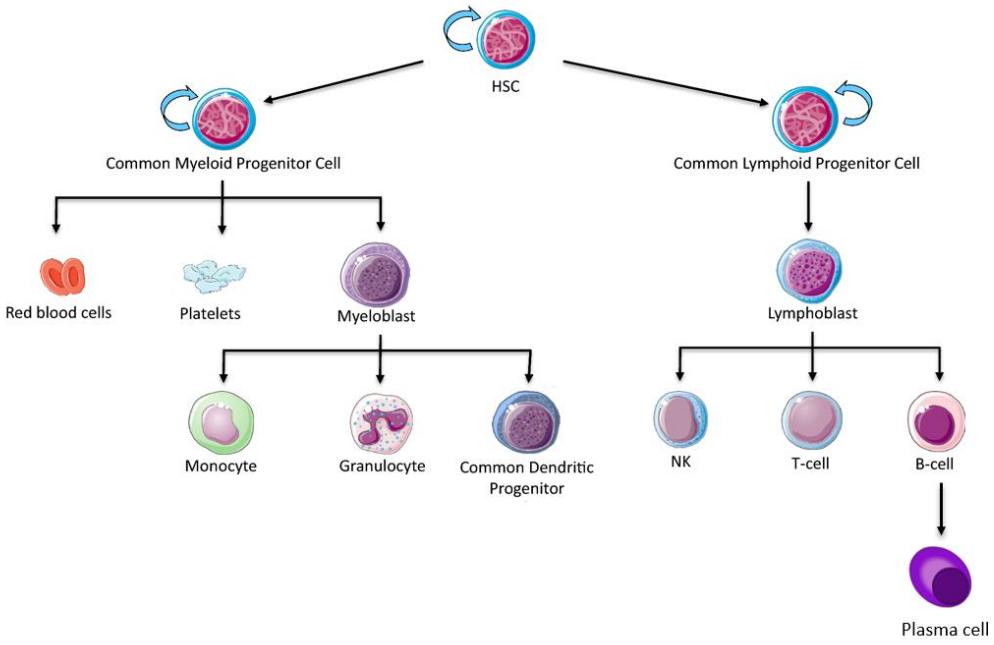

Figure 1 – Representative scheme of hematopoiesis. Hematopoietic stem cells are multipotent progenitors capable of give rise to both myeloid and lymphoid cell lineages. Myeloid cells derive from a common myeloid progenitor lineage whose differentiation give rise to several cell-types. A common lymphoid progenitor originates crucial cellular components of the immune system such as B, T, and natural killer cells. B cells, through a series of differentiation events, results on the formation of plasma cells. [Adapted from Rocamonde, B., *et al.* (2019)]

Particularly, B lymphocytes are a critical component of our immune system, which is responsible for our organism's defense and protection. A hierarchically regulated network of transcription factors, involving PU.1, E2A, early B-cell factor 1 (EBF), and paired box 5 (PAX5), controls the onset of early B cell development (Figure 2)[5]. These transcription factors are required not only for B cell maintenance, but also for the rearrangement of immunoglobulin variable-region genes, which is a vital phase in B cell diversity. The naïve B cells then self-renew and produce multipotent progenitors (MPPs), which develop into a common lymphoid precursor (CLP) or a common myeloid progenitor (CMP). Thus, early lymphoid progenitors (pre-proB cells) develop into irreversibly committed progenitor B (pro-B) cells, precursor B (pre-B) cells in the early stages of immunoglobulin rearrangement, and immature B cells[6,5].

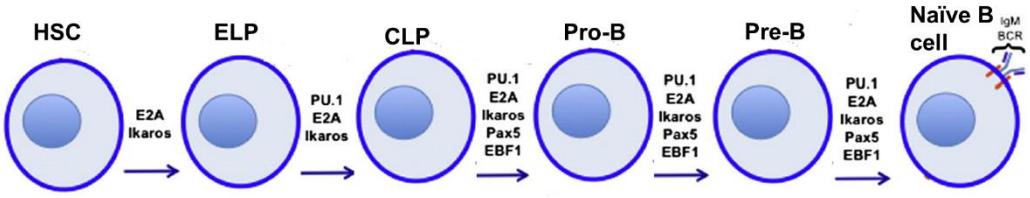

Figure 2 – B cell development in the bone marrow at a very early stage. The hematopoietic stem cell (HSC) stage initiates differentiation, originating early lymphoid progenitors (ELP). ELP differentiates into CLP that progresses on to the pro-B and pre-B stages. B cell development in the bone marrow is completed when the immature naïve B cell differentiates. Immature B cells express a full B cell receptor at this stage and exit the bone marrow to finish their development in the spleen. [Adapted from De, S. & Barnes, B. J. (2014)].

These naïve B cells originate more differentiated progenitors, eventually resulting in matured and differentiated blood cells expressing cell-surface immunoglobulin M (IgM) leaving the blood marrow and being transported to the spleen through the vascular system. Cells can re-enter the bloodstream, and when they come into contact with an antigen, they migrate to the lymph nodes, where they hypermutate and enhance the affinity of the antibodies generated. These centroblasts then begin to produce their antibodies and develop into centrocytes. The centrocytes undergo a selection process, turning into B clones that gained mutations that confer higher affinity antibodies towards the antigen. The B clones then receive a differentiation signal to develop as either memory B cells or plasmoblasts, that once in the bone marrow, mature into antibody secreting plasma cells[7].

The short half-life of the cellular components of the blood and their constant replacement and maturation turns hematopoiesis very prone to the build-up of genetic errors and, consequently, to the development of hematological malignancies. Lymphoid malignancies are a heterogeneous group of hematological neoplasms derived from the alteration of B, T, or natural killer cells at any stage of their development. The existing categorization of this broad cluster of hematological cancers reflects the maturity of the cell lineage concerned, the clinical progression of the disease and the presence of genetic alterations, mainly mutations and translocations[6].

2. Multiple myeloma

Multiple myeloma (MM) is a rare blood disease that accounts for 1% of all cancers and approximately 13% of all hematologic malignancies[8]. MM is characterized by expansion of clonal plasma cells (PC) that secrete monoclonal immunoglobulin (Ig) in the bone marrow (BM). These Igs circulate through the blood flow and accumulate in the organs causing them to decline their function[9]. The prevalence of the disease varies globally, although it peaks in more industrialized countries like the United States, Western Europe, and Australia[10]. The increasing frequency in developed countries is most likely due to the better diagnostic procedures and increased clinical awareness of the condition. Moreover, MM is two to three times more common in black citizens than in white individuals[11]. This malignant neoplasm primarily affects elderly people with the average age at diagnosis of about 70 years.

MM is included in a group of diseases known as monoclonal gammopathies and can be originated by an asymptomatic premalignant stage denominated monoclonal gammopathy of undetermined significance (MGUS) (Figure 3)[8]. The diagnosis of MGUS requires the absence of CRAB features[12]. The acronym CRAB summarizes the most typical clinical manifestations of multiple myeloma, these being hypercalcemia, renal failure, anemia, and bone disease. CRAB can be used to distinguish between active, symptomatic MM and MGUS[13]. This distinction is relevant not only for diagnosis but also for treatment. CRAB factors also effect the prognosis of MM. In fact, a study by Nakaya, A. *et al.* (2017) revealed that patients with hypercalcemia and bone disease showed a significantly worse prognosis, whereas anemia and renal failure showed no difference in survival[13]. The diagnostic criteria for monoclonal gammopathies have been amended to allow certain patients to begin therapy earlier (and consequently, achieving a better therapeutic outcome), mainly because of the increased recognition of biomarkers that can identify patients at high risk of progression to active illness (that is, multiple myeloma

that requires therapy). Nowadays, the diagnosis of MM is reliant on the present of more than one myeloma defining events. These myeloma defining events compromises on one or more established CRAB features accompanied by malignity biomarkers such as clonal bone marrow superior to 60%, serum free light chains ratio superior to 100, and at least one focal osteolytic lesion attained on magnetic resonance imaging examinations[14,15].

Furthermore, the application of genomic tools has led to a greater understanding of the underlying genetic abnormalities of multiple myeloma, both at a chromosomal and single gene level, indicating that multiple myeloma is a collection of diseases with a shared clinical pattern, rather than a single disease[8].

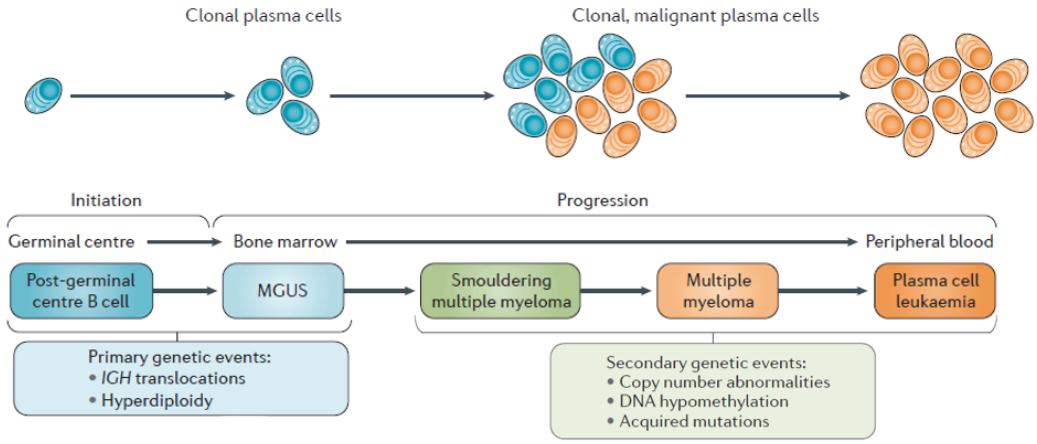

Figure 3 – Establishment of monoclonal gammopathies. The development of MM involves many steps, usually starting at MGUS. Genetic mutations and changes in the bone marrow microenvironment can originate smoldering MM. This stage precedes MM and if the tumor cells proliferate in the blood stream, plasma cells leukemia is originated. [Adapted from Kumar, S.K., *et al*. (2017)]

3. NF-κB signaling pathway

The activation of nuclear factor-kB (NF-κB), is thought to be a very common event in MM. Among the factors involved in inflammatory responses, NF-κB is one of the most important molecules that links chronic inflammation to cancer[16]. In fact, inflammation takes a crucial part in the development and the progression of most cancers. NF-κB is a family of transcription factors that modulates immune responses to bacterial and viral infections, inflammation and cell proliferation[17]. The NF-κB pathway is commonly known for its anti-apoptotic effects promoting cancer cells survival. Thus, it is essential in MM pathogenesis and can be constitutively active in MM[18]. Moreover, it was found that drug

sensitive MM cells display lower NF-κB activity when compared with drug resistant ones, and that NF-κB levels were higher in MM cells obtained from relapsed patients. Furthermore, the inhibition of the NF-κB pathway is one of the targets of bortezomib, leading to apoptosis of myeloma cells[19]. Elevated interleukin (IL)-6 production and NF-κB activation contribute to cancer progression and chemo-resistance[20].

NF-κB consists of the proteins Rel A (p65), Rel B, p50 (and its precursor p105), c-Rel and p52 (and its precursor p100). NF-κB is a homo or heterodimeric complex that usually consists on p65-p50 dimers. The dimers bind at kB sites in the DNA of their target genes. Different dimer groupings can act as transcriptional activators or repressors. NF-κB complexes are usually detained in the cytoplasm in an inoperable state associated with members of the NF-κB inhibitor (IkB) family such as IkBα, IkBβ, IkBγ, IkBε, p105, and p100[17].

In the traditional or canonical activation pathway [Figure 4, (a)], IkB is phosphorylated by IkB kinases (IKKs) due to different activators, such as tumor necrosis factor (TNF) α, IL-1β and bacterial lipopolysaccharide (LPS). The complexes are afterward degraded leading to the release of NF-κB in its active form which translocates into the nucleus[21]. The canonical NF-κB signaling pathway triggers the creation of p65\p50 and c-Rel\p50 heterodimers. The intensity and length of the NF-κB activity can be regulated by coordinating the degradation and synthesis of its components. Indeed, IKBα is encoded by a NF-κB target-gene[22]. Other NF-κB target genes encode for tumor inducing and inflammatory cytokines such as TNF, IL-1 and IL-6; for growth enhancing cytokines like IL-2 and for cell-adhesion molecules as ICAM-1. Additionally, some molecular factors whose expression is controlled by NF-κB, such as cyclin D1, can mediate cell cycle progression. Interestingly, NF-κB factors can trigger cell survival by promoting the expression of antiapoptotic genes that encode for proteins like BCL-2, BCL-XL, XIAP and survivin[23]. Moreover, the activation of the *MYC* gene is a molecular driver for the progression from the premalignant MGUS stage to MM. It can be found on chromosome 8q24. NF-κB triggers the expression of MYC (v-myc myelocytomatosis viral oncogene homolog, c-MYC) is a oncoprotein that was discovered in 1982 as a cellular homolog of the avian retroviral oncogene v-myc[24].

The alternative NF-κB pathway, that is induced by CD40 [Figure 4, (b)], by the lymphotoxin β receptor, and by B cell activating factor receptor[25], is crucial in lymphoid development and B cell maturation[26]. In this pathway, the instigation of IKKα homodimers leads to the activation of p52, that favorably dimerizes with RelB[27]. Then, this structure is translocated to the nucleus and acts as a transcription factor. Additionally, this pathway

also promotes p105 phosphorylation by the standard IKK complex, causing the ubiquitination, degradation and loosening of p50 homodimers that migrate into the nucleus inducing gene transcription. The IKK complex requires its regulatory subunit, NEMO (also known as IKK-γ), to function properly. Commonly to both pathways is that NF-κB promotes IkBα synthesis that, arriving in the nucleus, separates NF-κB from DNA, exporting the complex back to the cytoplasm re-establishing the initial state[28].

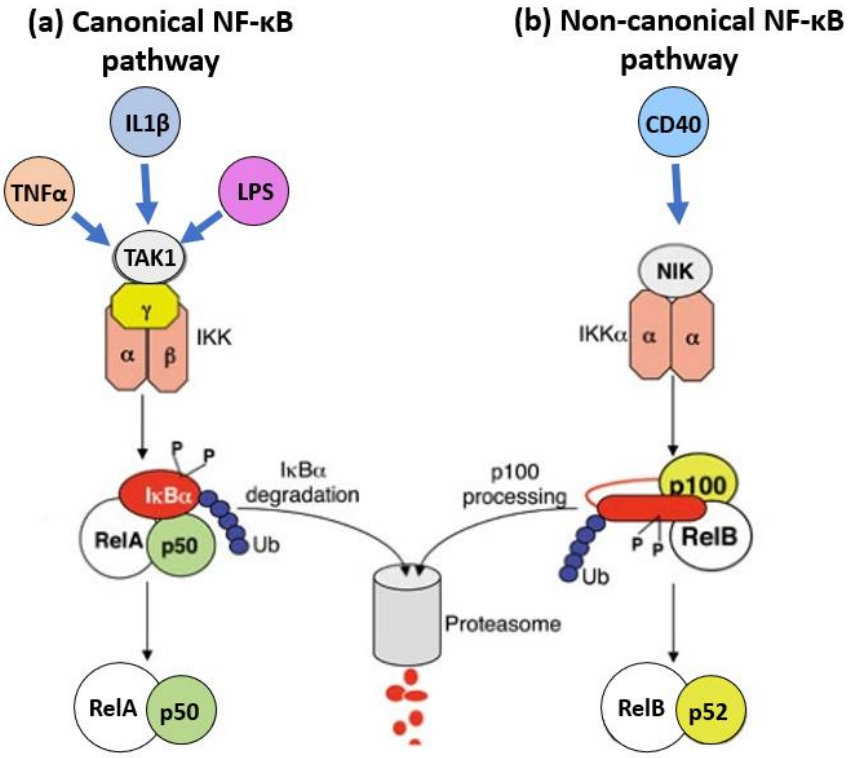

Figure 4 – NF-κB canonical and non- canonical pathways. Numerous signals, including those mediated by innate and adaptive immunological receptors (e.g., TNFα, IL1β and LPS) activate the classical route of NF-κB (a). It involves Tak1 activating the IKK complex, IKK-mediated IκBα phosphorylation, and subsequent degradation, culminating in the prototypical NF-B heterodimer p65/p50 translocating to the nucleus. Phosphorylation-induced p100 processing is activated by signals such as CD40 in the non-canonical NF-B pathway (b). This route mediates the persistent activation of the Rel B/p52 complex and is dependent on NIK and IKK. [Adapted from Sun, S. (2011)]

The Rel homology domain, which is about 300 amino acids long and contains sequences essential for DNA binding, dimerization, and inhibitor binding, connects the NF-κB proteins structurally[29]. The p105 protein is encoded by the *NFKB1* gene and is found on the human chromosome 4q24. The N terminus of p105 corresponds to NF-κB subunit p50. There is evidence that p50 is generated by the removal of the C terminal consensus sequence of p105 by the 26S proteasome[30]. Since p50 is a cleaved result of p105, it only has the DNA binding domain and must form a complex with p65, Rel B or c-Rel in order to perform as a transcription factor controlling gene expression[31]. On another hand, the *NFKB2* gene, located in 10q24.32, encodes for the p100 protein which just like p105, is cleaved by the proteasome, resulting in p52. The conversion of the NF-κB2 precursor protein p100 to p52 is a key step in the alternative NF-κB pathway's activation. The activation of NF-κB-inducing kinase (NIK) and IkB phosphorylation of

p100 at Ser 866 and Ser 870 is a critical molecular event in stimuli-induced p100 processing. This is necessary for the recruitment of E3 ligase b-transducin repeat containing protein to the p100 complex in response to stimuli, as well as the subsequent ubiquitination and processing of p100 to produce p52[32]. *REL* gene encodes for the protein c-Rel, which is an important gene transcriptional activator, that is primarily expressed in lymphoid and myeloid tissues. This gene is located in the chromosome 2p16.1, but it was found to be amplified on the human chromosome 2p14-15 on 23% of diffuse large B cell lymphomas[33]. The regulators of c-Rel include the inhibitors IkB and MALT1, which impair the formation of dimers and decrease c-Rel's nuclear migration. Just like p65 and p50, c-Rel also regulates cytokine production and plays a role in the development of T-cells. Moreover, c-Rel induces the expression of antiapoptotic genes[34]. *RELA* is a gene located on the chromosome 11q13 that encodes for a 65 kDa subunit of NF-κB called p65. In MM cells, this gene has been proved to be constitutively expressed[35]. This protein, just like c-Rel shows a high transcriptional activity. *RELB* gene, located in 19q13.32, encodes for the Rel B subunit. This NF-κB element cannot homodimerize and can only obtain it's transcriptional abilities when joined with p50 or p52[36]. Rel B can be negatively regulated by trapping in p65/Rel B or p100/Rel B complexes[37]. Rel B is crucial for the development of the bone marrow milieu and for the differentiation of dendritic cells[38]. Lastly the *IKBKB* gene, located in 8p11.21, encodes for the IKKβ protein. This kinase is crucial in the canonical activation of NF-κB. IKKβ is a catalytic subunit of the IKK complex that phosphorylates the IkBα inhibitor, causing it to be degraded by the proteosome[39]. A mutation on the *IKBKB* gene, resulting in the conversion of 171 lysine to glutamate was documented in MM patients[40].

A study conducted by Annunziata *et al.* (2007) concluded that NF-κB related genetic mutations are present in around 28% of MM cells, being *NFKB1* amplifications and *NFKB2* deletion noted by the authors[41]. According to following studies performed in MM cell lines, mutations can activate either the classical NF-κB pathway (for example, *NFKB1*, *CYLD, TACI* and *BCMA* mutations) or the alternative one (e.g., *NFKB2* mutations). TACI and BCMA are two cellular receptors shared by the soluble extrinsic factors APRIL (a proliferation-inducing ligand) and BAFF (B-cell activating factor). APRIL and BAFF are thought to exacerbate NF-κB's classical activity both in healthy and in cancerous plasma cells and they play a role in supporting their survival. Additionally, BAFF binds specifically to another receptor, BAFFR. On another hand, CYLD is a deubiquitinating enzyme that prevents NF-κB from becoming activated. Consequently, when mutations in the gene that encodes CYLD are present, NF-κB is activated. Moreover, the loss of CYLD's deubiquitinating function has been linked to

carcinogenesis[42]. The negative regulation of NF-κB by CYLD interaction with NEMO preventing IKB phosphorylation. Furthermore, CYLD can exert its deubiquitination abilities on TRAF2 causing the suppression of NF-κB[43]. Nevertheless, most NF-κB related genetic alterations trigger both pathways (for instance, *cIAP1/2*, *TRAF2* and *TRAF3* mutations)[44,45]. The predominancy of *TRAF3* mutations on MM cells might be elucidated by the occupation of *TRAF3* in chromosome 14 that is repeatedly found lacking in MM tumors[46]. Genetic abnormalities in the genes embodied in the last group results in augmented levels of NIK protein, for the reason that cIAP1/2, TRAF 2, TRAF 3 negatively regulates NIK. NIK levels are regulated by an interplay between TRAF 3 and TRAF 2 leading to the recruitment of the TRAF2-cIAP1/2 complex culminating in NIK's proteasomal degradation[47]. Consequently, mutations that cease *cIAP1/2, TRAF2* and *TRAF3* expression ends in NIK stimulation and in NF-κB 2 processing. Remarkably, high levels of NIK can set off the classical pathway alongside of the noncanonical. Effectively, NIK expression in distinct cell lines can start up both pathways through a NIK and IKKα reliant procedure[48].

4. Multiple myeloma treatment

Choosing the right treatment for a multiple myeloma patient is a complicated decision-making process, mainly as a result of the deeper understanding of plasma cell biology, which culminated in more therapeutic possibilities at each stage of treatment. Some treatment options for MM include proteasome inhibitors (PI), as bortezomib (BTZ), carfilzomib (CFZ) and ixazomib (IXZ), immunomodulatory drugs (IMiDs) as lenalidomide and pomalidomide, and monoclonal antibodies (MoAbs) as daratumumab and elotuzumab[9].

The 26S ubiquitin-proteasome pathway plays an essential role coordinating homeostasis and various cellular events including those involved in tumorigenesis[49]. This pathway is responsible for the degradation of intracellular proteins, which have been targeted for destruction by a protein called ubiquitin, through proteasomes. The 26S proteasome is an ATP-dependent protease that consists of two compartments: a 20S core particle (CP) and a 19S regulatory particle (RP) that caps one or both ends of the CP. Caspases, trypsins, and chymotrypsin-like catalytic activities are catalyzed in the CP by three catalytic sites, β1, β2, and β5 subunits, respectively. The pharmacological inhibition of proteasome function is useful as anticancer agents, since aberrant proteasome-dependent proteolysis has been associated with the pathophysiology of some malignancies, such as MM[49]. Therefore, aiming key features of protein function

responsible for the growth and development of cancer has been the focus of intense research. Misfolded or unfolded proteins gather in the endoplasmic reticulum (ER) once the proteasome is inhibited, creating ER stress. ER stress impairs cell cycle regulation, activates apoptotic pathways, and leads to cell death. Thus, proteasome inhibition leads to increased rates of apoptosis induction that is particularly significant in malignant cells[50,51]. Another possible route of PI-induced cellular damage is direct apoptosis induction via c-Jun NH2-terminal kinase (JNK) and p53. In fact, JNK induces cell death by triggering caspase-8 and caspase-3. Proteasome inhibition causes the accumulation and phosphorylation of p53, inducing pro-apoptotic proteins such as NADPH oxidase activator (NOXA) and BCL-2-associated X protein (BAX), which leads to apoptosis via mitochondrial failure[52].

Induction, consolidation, and maintenance are the three steps of the current therapy strategy for newly diagnosed MM. Typically, the first line of MM treatment consists of the association between bortezomib, lenalidomide and dexamethasone. This first drug regime is also known as induction therapy. This type of combination has been shown to have the higher response rate in MM patients eligible for transplant. The purpose of induction therapy is to minimize myeloma load, to alleviate symptoms, and to allow a successful stem cell collection. In order to facilitate stem cell collection and to avoid high toxicity levels, patients who are transplant candidates usually are not inducted for more than 4–6 cycles[53]. However, this initial therapy may be continued after stem cell harvest in patients who respond well and tolerate induction, saving autologous stem cell transplantation (ASCT) for the first MM recurrence. ASCT is generally followed by consolidation and maintenance therapy. This represents a brief course of chemotherapy that aims to improve ASCT results whilst extending MM's remission time. These regimens normally include bortezomib, thalidomide or lenalidomide[54]. Significantly, factors like comorbidities (decrease organ function), fitness, frailty syndrome, and age can make patients not eligible for transplant. In those cases, the therapy consists of combination regimes of bortezomib, melphalan and dexamethasone[55].

4.1 Proteasome inhibitors

4.1.1 Bortezomib

Bortezomib was the first proteasome inhibitor approved by the United States' Food and Drug Administration for the treatment of relapsed/refractory MM in 2005[56]. BTZ's

main mechanism of action in MM is the inhibition of the 20s chymotrypsin-like domain leading up to the blockage of the cell cycle and apoptosis through NF-κB signaling pathway suppression. In fact, this drug was firstly used in the treatment of refractory MM as an inhibitor of NF-κB as it prevents the proteasomal degradation of IkBα[51]. Bortezomib has been proved to reduce inducible NF-κB activity in MM cells, although its effect on constitutive NF-κB activity is yet to be determined. Yet, a recent study found that bortezomib enhances constitutive NF-κB activity in MM cells, implying that the effects of bortezomib on the NF-κB pathway in MM cells may vary depending on cell type and on the prevailing type of NF-κB pathway (canonical or non-canonical)[57]. BTZ also inhibits the expression of numerous cell adhesion molecules, including VLA-4, decreasing adhesion-mediated drug resistance[52]. Furthermore, BTZ shows a synergetic effect when administered with dexamethasone[58,59,60].

4.1.2 Carfilzomib

Carfilzomib (CFZ) is a next generation epoxyketone-based PI approved by the FDA in 2012 for the treatment of MM patients who've relapsed[61]. Carfilzomib binds irreversibly to the β5 subunit of the proteasome, leading to a potent inhibition of proliferation and induction of apoptosis. The approval of CFZ as a single agent was based in studies, similar to the one performed by Siegel *et al.* (2012) that showed higher response rates in relapsed MM patients[62]. Furthermore a study performed by Stewart *et al*. proved that the combination of CFZ with dexamethasone or with lenalidomide plus dexamethasone showed significant improvement of survival in relapsed patients[63]. Moreover, CFZ originates cardiovascular side effects. Not long ago, Efentakis *et al.* have found that CFZ's cardiotoxicity is linked to autophagic processes and to the augmentation of protein phosphatase (PP)-2A activity, although is it not related to the suppression of the proteasome function[64].

4.1.3 Ixazomib

Ixazomib (IXZ), the first oral PI, is a reversible boronate peptide that binds and inhibits the β5, β2 and β1 proteosome subunits. IXZ was originally approved for the treatment of relapsed and refractory MM in 2015[65]. As the other PIs, IXZ promotes caspase-dependent induction of apoptosis and inhibition of cell cycle, inhibits the NF-κB pathway in MM cells and inhibits tumor-associated angiogenic activity[9]. Interestingly, IXZ shows a superior tissue penetration and greater a biological activity compared to BTZ whilst being better tolerated, with a noticeably low toxicity profile[66]. The synergetic effect of IXZ, lenalidomide and dexamethasone was proved to significantly amplify the survival

of patients in relapsed and refractory MM[67]. Additionally, in newly diagnosed MM patients, IXZ also showed promising results[68].

In addition to PIs, other anticancer agents such as immunomodulatory drugs (IMiDs) (e.g. lenalidomide, and pomalidomide), and monoclonal antibodies (MoAbs) (e.g. daratumumab and elotuzumab) are also widely used in MM treatment[9].

5. Multiple myeloma's resistance mechanisms

MM patient's clinical course is characterized by relapses after several stages of therapy[69]. The main cause for the relapses is drug resistance, resulting from genetic and epigenetic alterations, abnormal drug transport and metabolism, decreasing the intracellular drug levels, dysregulation of apoptosis, activation of autophagy, persistence of cancer stem cells (CSCs) insensitive to most drugs or a dysfunctional tumor microenvironment, enlightened by the dependence of MM cells on the stromal microenvironment components (Figure 5)[70,71].

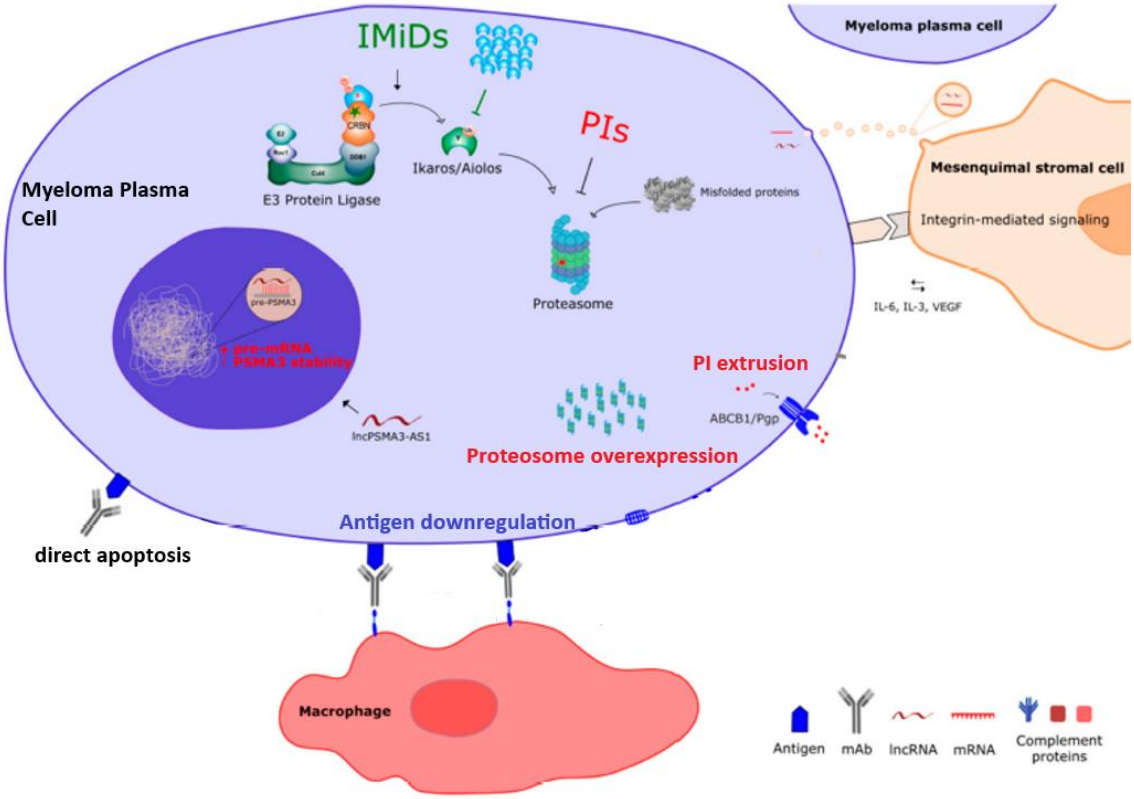

Figure 5 – Most common resistance mechanisms in MM. PIs, IMiDs, and the more recent MoABs, are the main chemotherapeutic agents used in MM treatment. Nevertheless, MM cells develop resistant mechanisms easily turning the drugs inefficient. Red lettering indicates

resistance to PIs, green letters indicate resistance to IMiDs, and blue letters indicates resistance to mAbs. [Adapted from Mogollón, P. *et al* (2019)].

5.1 Molecular mechanisms of resistance in MM cells

Despite the breakthroughs made in the discovery and development of new drugs for MM therapy, patients who have been treated for a long time often experience relapses and the disease can manifest itself more aggressively. This fact becomes much more frightening when one considers that malignant plasma cells have molecular mechanisms to protect them from cancer-fighting molecules like PIs and IMiDs[72]. The development of therapeutic resistance can take place in stages, beginning with uncommon cell transcriptional variability and progressing into stable epigenetic reprogramming. Malignant plasma cells become genetically unstable and produce extreme amounts of aberrant proteins. Genetic mutations and epigenetic modifications affecting genes like tumor suppressors, can be involved in the resistance mechanism[70].

Particularly, even though PI treatment has shown to be effective, primary, and secondary resistance are becoming increasingly common. In most individuals, long-term treatment with these drugs results in drug-resistant recurrence. The activity of the proteasome inhibitors bortezomib and carfilzomib is primarily directed at the β5 proteasomal subunit[51]. The most common genetic alteration found in the bortezomib-resistant cell lines was overexpression of the β5 subunit[73]. Also, the existence of point mutations in the *PSMB5* gene that codes for the β5 proteasomal subunit, resulting in spatial arrangement of the proteasomal catalytic site, is a likely cause for proteasome inhibitor resistance in MM[51].

Multidrug resistance (MDR) is another known mechanism of chemotherapy protection characterized by a low cellular capacity to accumulate drugs[74]. This fact is a result of the activity of an energy dependent, unidirectional, membrane bound drug efflux pump[51]. Drug efflux was found to be regulated by members of the ATP binding cassette (ABC) transporter family of proteins. P-glycoprotein (Pgp)/ABCB1 was the first ABC transporter reported. Currently, 49 distinct ABC transporters have been identified in humans. MDR is caused by the overexpression of certain ABC transporters in cancer cell lines and tumors, and it is a key promotor of chemotherapy failure. Membrane proteins belonging to the ABC transporter superfamily are able to export a wide range of substrates across cellular membranes leading to a reduction in intracellular drug concentrations[51,75].

As mentioned before, anticancer treatment is impaired when apoptosis is disrupted. Apoptosis signaling failure is a key oncogenic factor in MM resistance and it is commonly linked to BCL-2 family dysregulation[51]. MCL-1, a member of the BCL-2 family, is a key antiapoptotic factor that inhibits antiapoptotic signaling. MCL-1 levels are elevated in resistant MM cell lines, preventing cell death[76].

In summary, even though the agents that compose the backbone of MM treatment are effective, patients frequently develop drug resistance. Thus, the clinical available drugs may not be an option for them. For this reason, new anticancer agents, such as parthenolide, are needed in order to overcome drug resistance in relapsed/refractory MM.

6. Parthenolide

Parthenolide (PTL) is a sesquiterpene lactone (SL) initially purified from the shoots of feverfew (*Tanacetum parthenium*), has powerful anticancer and anti-inflammatory proprieties[77]. PTL belongs to the SL family of plant secondary metabolites; thus, it has a 15-carbon (15-C) structure comprising three isoprene (5-C) units and a lactone group (cyclic ester) (Figure 6)[78]. This compound is currently being tested in cancer clinical trials. Structure-activity relationship (SAR) studies of parthenolide uncovered crucial chemical characteristics mandatory for biological activities, and led to the development of an analog, dimethylamino-parthenolide (DMAPT). Parthenolide is the first small molecule found to be selective against CSCs[79].

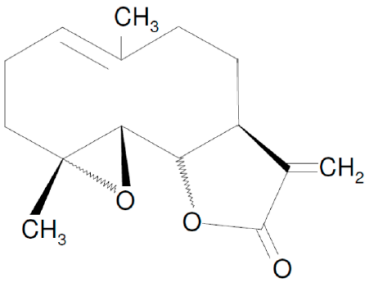

Figure 6 – Chemical structure. PTL belongs to the SL family of secondary plant metabolites. It has a 15-carbon (15-C) structure comprising three isoprene (5-C) units and a lactone group (cyclic ester). [Adapted from Sztiller-Sikorska, M. *et al* (2020)].

Due to its anti-inflammatory proprieties, feverfew has been utilized for hundreds of years to relieve arthritis pain, while being also an anticoagulant, a digestive, an insect repellent, an initiator of uterine contractions during childbirth and of menstruation, and as treatment for depression, vertigo, kidney stones, infant colic and skin wounds[79].

However, commercially available PTL for research has been extracted from *Chrysanthemum parthenium* leaves. In 1973, PTL was shown for the first time to have antitumor properties[80]. These biological abilities of PTL is the result of its inhibition of NF-κB, primarily described in 1997[81], by aiming numerous steps along the NF-κB signaling pathway[82]. Actually, PTL is frequently sold as a pharmacological NF-κB inhibitor although it also targets epigenetic factors, inhibits the Janus kinase/signal transducers and activators of transcription (JAK/STAT) pathway and leads to cellular oxidative stress by reactive oxygen species (ROS) formation[78]. The significant role that PTL can play in cancer therapy is often restricted by secondary effects, especially at elevated doses, and high hydrophobicity, which reduces the oral bioavailability and solubility of the drug in blood plasma[79].

PTL is a well-known NF-κB suppressor as it has the capacity to target numerous elements of the pathway. Contrarily to most NF-κB inhibitors, the structure of PTL does not offer radical-scavenging activity[81]. Quantitative SAR linked PTL's inhibitory potential with the number of alkylating centers, such as the methylene lactone and conjugated keto or aldehyde functions. In fact, the presence of an α-methylene-γ-lactone center was the most vital condition for NF-κB inhibition[83]. Another study, using PTL derivatives, discovered that more-polar molecules, bearing hydroxyl groups, are stronger inhibitors of NF-κB, perhaps owing to hydrogen bonding with amino acid residues next to the target cysteine in NF-κB[83]. Parthenolide inhibits the NF-κB pathway by directly binding to NF-κB subunits. The exomethylene group of PTL inhibits DNA binding of the p65/NF-κB subunit by alkylating p65 cysteine-38, which is decisive for hydrogen bonding with DNA[84].

SLs missing the exomethylene group do not constrain NF-κB even at very high concentrations. It is also interesting to note that p65 point mutations, in which occurs the replacement of cysteine-38 by serine, cancels the inhibition of NF-κB by PTL. Furthermore, PTL with extra free cysteines eliminates its NF-κB inhibitory potential[81-85]. Nevertheless, not all cysteines are targeted by PTL, for instance, p65 cysteine-120 defends against the inhibitory potential[85]. PTL can inhibit the IKK complex, another target in the NF-κB pathway, leading to proteasomal degradation[86]. However, NF-κB DNA binding can be completely inhibited by PTL with no effect on IKK. An effect on IκB might be observed at higher PTL concentrations, masking the effect on p65, which is preferentially induced at lower concentrations[85].

6.1 Anticancer mechanisms of PTL *in vitro*

PTL modulates signaling pathways that provide it with specific cytotoxicity to numerous tumor types *in vitro*. The underlying molecular interactions are linked mainly to the ability of PTL to inhibit NF-κB, AP-1, mitogen-activated protein kinase (MAPK), and/or JNK and redox stress, ultimately resulting in gene expression changes, essentially downregulating anti-apoptotic and upregulating pro-apoptotic genes (Figure 7)[78,87].

Furthermore, PTL also is an effective inhibitor of STAT proteins. It is known that STAT3 expression contributes to resistance to chemotherapy and radiotherapy in several types of cancer as it binds to DNA sequences in target genes that encode frequently for anti-apoptotic proteins, for proteins that prevent cell cycle arrest, and for proteins that promote cell proliferation[88]. By blocking STAT3 phosphorylation on Tyr705, PTL prevents STAT3 dimerization, its nuclear translocation, and STAT3-dependent gene expression[89]. Several STAT3 inhibitors show antitumor activity and inhibit STAT3 phosphorylation but are yet to be approved for clinical cancer therapy[88].

PTL's therapeutic benefits are also aided by oxidative stress. PTL-induced apoptosis is preceded by a drop in intracellular thiol levels, including both free reduced glutathione (GSH) and protein thiols, as well as the formation of ROS[90].

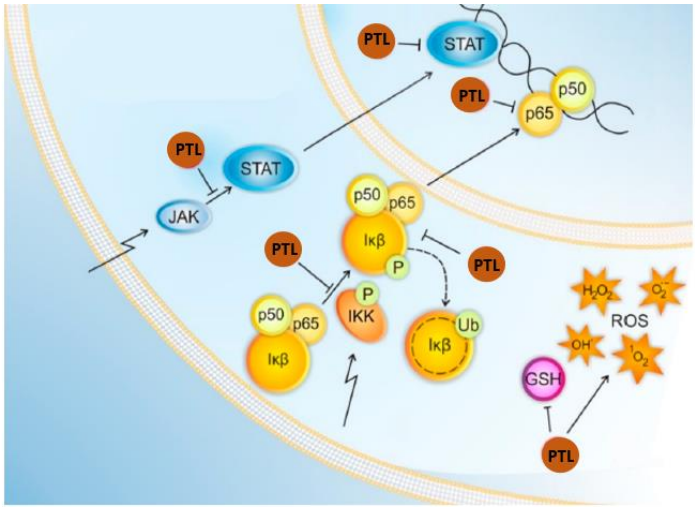

Figure 7 – PTL's mechanisms of action. PTL inhibits the NF-κB signaling pathway, by either interacting directly with the p65 subunit or by suppressing IKK. Additionally, PTL inhibits STAT3 phosphorylation preventing its nuclear translocation and STAT3-dependent gene expression. PTL also reduces cellular level of glutathione and causes the accumulation of ROS, inducing oxidative stress. [Adapted from Sztiller-Sikorska, M. et al (2020)].

As mentioned before, the chemotherapeutic properties of PTL were also attributed to its impact on epigenetic mechanisms which are often modified in cancer. Another role for PTL in cancer is its ability to modify DNA methylation. Countless tumors express high levels of DNA methyltransferases such as DNMT1 and DNMT3b, both of which lead to tumor progression by inhibiting the expression of tumor suppressor genes[91]. PTL leads to DNA hypomethylation *in vitro* and *in vivo* by inhibiting DNMT1 in myeloid leukemias and skin cancer[91]. Also, PTL specifically depletes histone deacetylase HDAC1 protein that has a role in chromatin remodeling[92]. The discovery of new epigenetic regulators such as PTL is indispensable to the application of epigenetic therapies.

7. Objectives

MM is a rare blood disease that is typically managed by using anti-cancer agents like PIs, IMiDs and MoAbs which have dramatically improved the quality of life of the patients. However, MM remains incurable mainly due to drug-resistance, therapeutic failure, and subsequent disease relapse. Therefore, the clinical existing drugs turn out not being a possibility for MM patients. Hence, new anticancer agents, such as PTL, are needed to surmount drug resistance in relapsed/refractory MM.

In this context, the major goal of the present project is to assess the role of parthenolide in circumventing multiple myeloma resistance to proteasome inhibitors BTZ, CFZ, and IXZ.

Materials and methods

1. Cell culture

1.1 Cell lines description and maintenance

In this study, the NCI-H929 cell line and three PI resistance cell lines were used. NCI-H929 was purchased from the American Type Culture Collection (ATCC). The H929 cells were originally obtained from a malignant effusion occurred in 62 years old caucasian woman with myeloma[93]. These cells grow in suspension in Roswell Park Memorial Institute 1640 medium containing 2 mM L-glutamine, 20 mM of HEPES-Na, 1,5 g/L of NaHCO3, supplemented with 2-mercaptoethanol at a final concentration of 0.05 mM and 20% of fetal bovine serum (FBS). Also, the cell medium is supplemented with ZellShield (Minerva Biolabs) to prevent bacteria, fungi, yeast, and mycoplasma contaminations. The cells were incubated at 37ºC in a humidified atmosphere containing 5% CO_2. The PI-resistant MM cell lines were established in the FMUC Laboratory of Oncobiology and Hematology by continuous exposure of H929 cells to bortezomib (H929-BTZ), carfilzomib (H929-CFZ), and ixazomib (H929-IXZ). In order to maintain a culture of the resistance cell lines, it is necessary to add to the culture medium the drug that the cells are resistant to. H929-BTZ grow with a concentration of 3nM of BTZ, H929-CFZ reach an optimal growth rate at a concentration of 2,5nM of CFZ, and H929-IXZ grow with a concentration of 20nM of IXZ.

The degree of resistance of the cell lines was calculated as the number of times it is needed increase the dose of a drug in a resistant cell line to obtain the same effect as in the parental line after 72 hours of incubation. H929-BTZ needs 5 times more BTZ than the parent sensitive line. In the same way, H929-CFZ demands for 6 times more CFZ than the parent sensitive line for the same therapeutic effect to be observed. H929-IXA needs 14 times more IXZ than the parent sensitive line.

1.2. Cell culture for the assessment of cellular density and viability

Firstly, sensitive and resistant cell lines were exposed to Trypan Blue (TB) in order to count cells and to assess cell viability. This method was proposed by Paul Ehrlich over a century ago and is still the most widely used method to perform cell viability analysis. Furthermore, the standard approach to estimate cell population density is to use TB with a hemocytometer. TB is a cell membrane-impermeable molecule and consequently it only enters the cells with a deteriorated membrane, meaning, dead cells[94]. Upon entry into the cell, TB binds to intracellular proteins and the dead cells are marked as blue whereas the color of living cells remains unchanged. However, the usage of TB shows

numerous disadvantages: TB exerts a toxic effect on cells after a short exposure period, it can bind non-specifically, it presents a big number of false positives (like “dead cells” resulting from irreversible damage to their membrane and not from apoptosis\necrosis) as well as false negatives (from cells that are already undergoing apoptosis but still have intact membranes), and lastly, cell counting is very time-consuming and operator-dependent process[95].

In order to assess the optimal cellular density to achieve the best growth rate, cells were cultured in a 48 wells plate at the initial density of $0.1x10^6$, $0.3x10^6$, $0.5x10^6$, $0.75x10^6$, $1x10^6$, $1.25x10^6$, and $1.5x10^6$ cells/mL. In this project, cells were incubated with TB and read in an automated cell counter (Invitrogen Countess 3 FL Automated cell counter), every 24 hours, for 96 hours, in order to estimate the optimal initial cell density to achieve the best cell growth. In order to assess the optimal cellular density to achieve the best growth rate, cells were cultured in a 48 wells plate at the initial density of $0.1x10^6$, $0.3x10^6$, $0.5x10^6$, $0.75x10^6$, $1x10^6$, $1.25x10^6$, and $1.5x10^6$ cells/mL. In this project, cells were incubated with TB and read in an automated cell counter (Invitrogen Countess 3 FL Automated cell counter), every 24 hours, for 96 hours, in order to estimate the optimal initial cell density to achieve the best cell growth. It was possible to conclude that the optimal initial cell density to achieve the best cell growth rate is 0,5 x 10^6 cells. It was also verified that after 72 hours cell viability significantly decreases because of the lack of space and nutrients.

1.3. Cell culture for the assessment of cellular metabolic activity

The next step of this project was to assess the metabolic activity of sensitive and resistant cell lines incubated in the absence and in the presence of various concentrations of PTL, by the resazurin assay. This compound, discovered by Weselsky in the 1920’s, is an indicator of cellular metabolic capacity. Primarily, it was valuable to evaluate bacterial and yeast contamination of milk. Nowadays, this redox dye is a marker of metabolic activity in cellular cultures. The resazurin assay is dependent on the intracellular reduction of resazurin to resorufin by viable, metabolically competent cells, usually being NADH and NADPH the electron source[96]. Resazurin is also reduced to resorufin by dehydrogenases[97]. This assay is extremely reliant on the temperature, pH, and initial resazurin concentration, subsequently, these parameters need to be kept constant throughout incubation and measurement[98].

In order to assess cellular metabolic activity, cells were cultured in a 48 wells plate at the initial density of $0.5x10^6$ cells/ml. Sensitive and resistant cell lines were incubated with PTL at the concentrations of 0.5, 1.0, 2.5, 5.0, 7.5, 10.5, 25.0 and 50.0 µM. At every 24 hours of incubation, over the course of 72 hours, a volume of resazurin (Sigma-Aldrich) at 0.02 mg/mL equivalent to 10% of the volume of cells was added. After about 5 hours of incubation with the dye, the intensity of reduced resazurin was measured at 600 and 570 nm on a microplate spectrophotometer. The metabolic activity on each condition was calculated according to equation 1:

$$Metabolic\ Activity\ (\%) = \frac{A_{[570-600]}\ Sample - A_{[570-600]}\ Blank}{A_{[570-600]}\ Control - A_{[570-600]}\ Blank}$$, equation 1.

2. Evaluation of cell death

Given that resazurin does not provide information on cell death and that apoptotic and necrotic cells are not distinguished by TB, cell death was evaluated in depth by flow cytometry (FC), using Annexin V (AV) and 7- amino antimycin D (7-AAD) double staining. Flow cytometry is a technique that uses the forward (forward scatter) and lateral (side scatter) light dispersion emitted by a light source (laser) and the fluorescence emitted by fluorochromes bound to monoclonal antibodies or other compounds to analyze and quantify cells or other biological particles[99].

Cellular decay takes place in two distinct ways, apoptosis and necrosis[100]. Apoptosis is a programmed and physiological manner of cellular death that plays a crucial role in the homeostasis of tissues. AV is a protein that, in the presence of calcium, binds to negatively charged phospholipids, like phosphatidylserine (PS). PS is normally situated in the inner membrane, but, when apoptosis is induced, PS migrates to the outer cell membrane and becomes exposed to AV[101].

Differently from apoptosis, necrosis is an unregulated process affecting a large number of cells. Necrotic cell injury is mediated by two main mechanisms: meddling with the energy supply of the cell and destruction to cell membrane. This loss of cell membrane integrity results in the release of the cytoplasmic contents into the surrounding tissue, sending molecular signals which leads to the recruitment of inflammatory cells[102].

Hence, AV principally binds to the external membrane of apoptotic cells. On another hand, 7-AAD is a DNA intercalating agent. It is excluded by the plasma membrane of living cells and trapped by dead cells. In necrotic cells, the membrane becomes permeable and molecules such as 7-AAD enter the cell and binds to the

DNA[103]. Therefore, this assay discriminates between viable cells (not stained with neither of the compounds), early apoptotic (stained with AV but not with 7-AAD), late apoptotic/necrotic (stained with both compounds), and necrotic cells (stained with 7-AAD but not with AV).

To evaluate the type of cell death 1 million cells were collected and centrifuged at 1000xg for 5 min with cold PBS (0.01 M, pH 7.4). The pellet was resuspended in 100 µL of cold binding buffer and incubated with 2.5 µL of Annexin V-APC (Biolegend) and 7.5 µL of 7-AAD (Biolegend) for 15 minutes in the dark, according to manufacturer's protocol. After incubation time, 300 µL of binding buffer were added and the analysis was run on a FACS Calibur flow cytometer (Becton Dickinson, San Jose, CA). Results were shown as a percentage of each of the recognized cell populations, based on the positivity and/or negativity for the dual labeling with annexin V and 7-AAD, ± SEM of 4 independent experiments.

Adding to the above stated flow cytometry assays, morphological studies were conducted to evaluate the morphological changes induced by exposure to PTL using the May-Grünwald Giemsa protocol and to distinguish between live and dead cells. This technique is a combination of two stains (May- Grünwald stain and Giemsa stain). The May-Grunwald solution combines the action of two dyes, eosin (acidic) and methylene blue (alkaline) whilst the Giemsa stains contains azure (alkaline). Azure and methylene blue, since they are basic compounds, they color the acid nucleus blue/purple. Eosin is an acidic dye that is attracted to the cytoplasm, which is alkaline, creating a reddish colouring[104].

Apoptosis involves the activation of caspases that cleave several structural proteins in the nucleus and cytoskeleton and trigger specific death-promoting nucleases. The apoptotic cell loses structural integrity and undertakes numerous morphological changes, for example condensation of chromatin, cleavage of nuclear DNA, shrinking of the cytoplasm and organelles, blebbing of the cellular membrane, and fragmentation of the cytoplasm into apoptotic bodies. Some of the major morphological changes that occur with necrosis include cell swelling; formation of cytoplasmic vacuoles; distended ER; ruptured mitochondria; disaggregation and detachment of ribosomes; disrupted organelle membranes; swollen and ruptured lysosomes and eventually disruption of the cell membrane[105].

For the morphological studies, 1 million cells were collected from each cell line and centrifuged at 1200 × g for 5 minutes. Subsequently, the cells were washed with PBS

and centrifuged again under the same conditions. To improve cell adhesion to the slides the pallets obtained from the centrifugation were resuspended in FBS before smearing. After drying, the smears were stained for 3 minutes with May Grünwald (Sigma-Aldrich) that was diluted with distilled water, in the proportion 1:1. Then, Giemsa solution was added, in the proportion of 3 ml of Sigma-Aldrich stock per 10 ml of ultrapure water for 15 minutes. The smears were washed and after these had dried, the morphology of the cells was analyzed under a Nikon Eclipse optical microscope 80i, coupled with a Nikon DXm 1200F digital camera to attain the images at 50X ampliation.

3. Evaluation of the effect of PTL in the mitochondrial membrane potential

Apoptosis is the reason behind many major cellular events, one of which being the loss of mitochondrial membrane potential ($\Delta\psi_M$)[106]. Throughout the life of a cell, the mitochondria utilizes oxidable substrates to establish an electrochemical proton gradient across its membrane. This gradient leads to the production of ATP[107]. Yet, during apoptosis, $\Delta\psi_M$ declines as permeability pores open in the mitochondrial membrane, thus, the electrochemical gradient is lost. So, $\Delta\psi_M$ is a critical limitation of mitochondrial vitality and it can be easily used as an indicator of cell viability.

FC assays using the JC-1 probe can assess the $\Delta\psi_M$ in mitochondria. In fact, the JC-1 dye is a lipophilic, green, cationic and fluorescence dye which can go into the mitochondria where it forms reversible complexes called J-aggregates. These J-aggregates emit fluorescence in the red spectrum instead of green. In competent cells, the JC-1 dye enters the negatively charged mitochondria and originates red fluorescent J-aggregates. Contrarily, in apoptotic cells, the augmented mitochondrial membrane permeability leading to the loss of electrochemical potential, causes the mitochondria to be less negatively charged. Hence, JC-1 does not have enough influence to trigger the formation of J-aggregates, so the mitochondria remain fluorescent green. Based on these premises, the green/red fluorescence ratio of the dye in the mitochondria can assess directly of the state of the mitochondria polarization. This means that the lower the $\Delta\psi_M$, the higher is the green to red ratio (less J-aggregates are formed). Therefore, the loss of mitochondrial membrane potential is designated by the increase in the green to red fluorescence intensity ratio[108].

After 72 hours of incubation, a volume equivalent to 1 million cells was collected and washed twice by centrifugation with PBS for 5 minutes at 300xg. Cells were

resuspended in 1 mL of PBS and incubated with 1 µL JC-1 (Molecular Probes, Invitrogen) dissolved in DMSO at 5 mg/Ml to give a final concentration of 5 µg/mL, for 15 minutes at 37ºC in a 5% CO_2 atmosphere. Subsequently, the cells were centrifuged with PBS by for 5 minutes at 200xg and resuspended in 400 µL of PBS. Analysis was performed on a FACS Calibur flow cytometer (Becton Dickinson, San Jose, CA) being that monomeric form (M) exhibited green fluorescence at the wavelength of 525 nm and the j-aggregates (A) were detected at the wavelength of 590 nm. Hence, $\Delta\psi_M$ was estimated by the ratio of green and red fluorescence intensity, that is, by the M/A ratio. The results represent the JC-1 M/A ratio mean ± SEM of 3 independent experiments.

4. Evaluation of peroxides

The outcome on cell death brought up by PTL through oxidative stress was evaluated using a fluorescent probe that allow the detection of ROS (peroxides).

2',7'-dichlorodihydrofluorescein diacetate or $DCFH_2$-DA is an ester compound that is capable of crossing the cell membrane. In the cytoplasm, it is hydrolyzed by enzymes called esterases in 2',7'-dichlorodihydrofluorescein ($DCFH_2$) becoming trapped inside the cell. When in contact with ROS, namely hydrogen peroxide (H_2O_2), it is oxidized in 2',7'-dichlorofluorescein (DCF), which emits green fluorescence upon excitation[109].

After 72 hours of incubation, a volume equivalent to 1 million cells was collected and washed twice by centrifugation with PBS for 5 minutes at 300xg. Cells were resuspended in 1 mL of PBS and incubated with 5 µL of DCFH2-DA (Molecular Probes, Invitrogen) dissolved in DMSO at 1 mM to give a final concentration of 5 µM for 45 minutes at 37ºC in a 5% CO_2 atmosphere. Subsequently, the cells were centrifuged with PBS by for 5 minutes at 200xg and resuspended in 400 µL of PBS. Analysis was performed on a FACS Calibur flow cytometer (Becton Dickinson, San Jose, CA) equipped with a laser using the wavelength of 525nm. The results are expressed as the mean of intensity of fluorescence that signifies the intracellular concentration of peroxides in the sensitive and resistant cell lines ± SEM of 3 independent experiments.

5. Cell cycle analysis

Cell cycle analysis was performed by FC, using propidium iodide/RNAse solution. As previously said, propidium iodide is a fluorescent dye that stains DNA in permeable cells. The fluorescence intensity, read by FC, is proportional to the DNA quantity of each

cell, permitting us to discriminated between cells in the G_0/G_1 phase (fewer amount of DNA), S phase (equivalent with the replication of DNA) and G_2/M phase (where the amount of DNA is the double of the G_0/G_1 phase). Also, cell death can be studied through this assay assuming that apoptotic cells account with the fewest DNA quantity as a result of DNA disintegration. Hence, a peak (sub G_0/G_1 or apoptotic peak) of fragmented DNA can appear before the G_0/G_1 phase.

Nevertheless, propidium iodide also binds to RNA so, with the purpose of having optimal DNA resolution, it is necessary to eliminate the RNA using the RNAse solution[110].

For cell cycle assessment, 1 million of cells were collected and washed with PBS for 5 minutes at 1000xg. Then, the cells were fixed by adding 200 µL of ice cold 70% ethanol, while being agitated on a vortex. After the incubation time of 1 hour at 4°C, the cells were centrifuged with PBS and then resuspended in 400 µL of propidium iodide/RNAse solution (Immunostep). Cells were then analyzed on a FACSCalibur flow cytometer (Becton Dickinson, San Jose, CA). The obtained results signify the percentage of cells in the different cell cycle stages (Sub G1, G0/G1, S, and G2/M) ± SEM of 4 independent experiments.

6. Gene expression analysis

In order to describe the gene expression of the four cell lines used, the NF-κB related genes *REL*, *RELA*, *RELB*, *NFKB1,* and *IKBKB* were evaluated by quantitative PCR or qPCR. Additionally, to evaluate the effect of PTL on gene expression, the expression levels of *BCL-2* and *MYC* genes were also assessed using the same strategy.

Initially, after a 72h incubation 3 million cells were collected and washed twice with PBS for 5 minutes at 1000xg. The supernatant was discarded, and the pallet was resuspended in 1ml of TripleXtractor (GRiSP) according to manufacturer´s protocol. TripleXtractor, is a ready-to-use monophasic solution of phenol and guanidine isothiocyanate, that has a powerful lysis ability that leads to cellular disruption and to the disbanding of cellular elements, while maintaining RNA integrity. Next 0.2 mL of chloroform per 1 mL of TripleXtractor were added. The tube was shaken in a vortex and, after 5 minutes at room temperature, it was centrifuged at 12.000xg at 4˚C for 15 minutes. The addition of chloroform results in a separation of layers forming a clear upper aqueous layer (containing RNA), an interphase, and a red lower organic layer (containing DNA, lipids and proteins). The aqueous phase was transferred to a new tube and the

RNA is precipitated by adding 1 volume of isopropanol per 1 volume of TripleXtractor applied. The tube was inverted and incubated at room temperature for 10 minutes. After that, another centrifugation took place at 12.000xg at 4ºC for 10 minutes. After the exclusion of the supernatant the pellets were then washed twice by adding 1 mL of 70% ethanol and gently inverted. The tubes were centrifuged at 12.000xg at 4ºC for 5 minutes. After the final washing step, the ethanol was discarded, and the pallets were air-dried with the intention of eradicate trace amounts of ethanol. The RNA pellet was then dissolved in RNase-free water and incubated at 60˚C for 10 minutes. The isolated RNA was stored at -80˚C in order to be used later.

After extraction, RNA was quantified using a Nanodrop spectrophotometer. The purity of the isolated RNA was assessed by the ratio 260 nm/280 nm. This quotient verifies the contamination of the sample by DNA and proteins since nucleic acids and proteins have maximal absorbance at 260 and 280 nm, respectively. An A260/A280 ratio of 1.8–2.1 at pH 7.5 is widely accepted as indicative of highly pure RNA[111,112]. Another important ratio to assess the purity is A260/A230, which value should be around 2 or slightly above; however, there is no consensus on the acceptable lower limit of this ratio. This proportion confirms the contamination of the sample by carbohydrates[113]. For the quantification a volume of 2 µL of each sample was employed.

Next, the isolated RNA was converted into cDNA using the Xpert cDNA Synthesis Master-mix Kit (GRISP). This kit has the enzyme reverse transcriptase which is able to produce cDNA complementary to the RNA.

First, in a RNase-free microtube it was mixed RNA template, mastermix (10 µL) and RNase free water. The volume of RNA used was calculated based on the RNA quantity acquired after quantification. The mastermix has the optimized concentration of oligo(dT) and random hexamer primers, deoxyribonucleotides (dNTPs), and RNase inhibitor. The volume of RNase free water added depended on the volume of RNA necessary.

Using a thermocycler (T100 Thermal Cycler, Bio-Rad) the tubes were warmed for 5 minutes at 65ºC, to eliminate potential secondary RNA structures, and then placed on ice for 2 minutes. Next, 1 µL of Xpert Reverse Transcriptase (Xpert RTase) was added. Xpert RTase is a DNA polymerase suitable for cDNA synthesis from long RNA templates. It operates under high temperatures enabling the exclusion of secondary RNA structures. Likewise, the absence of RNase activity guarantees minimization of template degradation.

The microtubes were then mixed, centrifuged and incubated at 25ºC for 10 minutes. Finally, using a thermocycler (T100 Thermal Cycler, Bio-Rad), the tubes were heated for 50 minutes at 50ºC and 5 minutes at 85ºC. The cDNA concentration was standardized to 50 ng/µL and then stored at -20ºC for later use.

The produced cDNA was then used to perform qPCR. This method uses a fluorescent dye called SYBR Green that binds to double-stranded DNA. The subsequent DNA-dye complex is capable of absorbing blue light and emitting green light, being proportional to the concentration of amplified double-stranded DNA. This precise probe allows the measurement of the fluorescence after each PCR cycle producing a real-time calculation of the concentration of double stranded amplified DNA fragments[114].

PCR was completed applying GRS Taq DNA polymerase (GRiSP). GRS Taq DNA polymerase is a thermostable that holds 5´→3´ polymerase action as well as weak 5´→3´ exonuclease activity. PCR starts with a DNA template and uses primers to selectively amplify a specific DNA fragment of interest. To execute a PCR reaction the needed reagents are: a DNA template, a pair of primers that hybridize with the DNA template, dNTPs (A, T, G, C) to build new DNA molecules, and a thermostable DNA polymerase, an enzyme that adds nucleotides to the forming DNA strand.

The first step of PCR consists of DNA denaturation, which is achieved by high temperature (95 °C for 5 minutes), allowing each strand to serve as a template. In the next phase hybridization of primers occurs. The solution is abruptly cooled to around 60°C to allow each primer to bind to a DNA strand. The primers bind to opposite ends of the opposite strands so that the region between the primers is amplified.

Finally, the solution is heated to the optimal temperature of the DNA polymerase. The polymerase extends both primers, as new dNTPs are added to the 3′ end of each primer. These three stages establish one cycle of PCR. In this case 35 cycles were carried out, where each cycle doubled the quantity of DNA from the former. The process was carried out by using T100 Thermal Cycler (Bio-Rad) thermocycler[115].

The values of expression of were obtained by comparing the cycle threshold (CT) value (which is the cycle number from which the fluorescence of the qPCR enters the exponential phase) of the target gene, with the CT value of an endogenous control gene (in this case it was *GUS B*). Because the efficacy of the endogenous control gene was higher than the efficacy obtained in most of the target genes, the expression level of the *REL*, *RELA*, *RELB*, *NFKB1, IKBKB, c-MYC* and *BCL-2* genes was calculated by the Pfaffl method, elucidated by equation 2.

$$expression = \frac{(E\ target)^{\Delta CT\ target\ (endogenous\ control\ gene-target)}}{(E\ ref)^{\Delta CT\ ref(endogenous\ control\ gene-target)}}$$, equation 2.

In equation 2, E target and E ref represent the efficacy of the amplification of the target and of the endogenous control gene, respectively. Also, ΔCT target and ΔCT ref equal to the CT of the endogenous control gene minus the CT of the target gene.

Data quality control is a crucial part of qPCR experiments. To assess the quality of the assay, the melting and standard curves of each sample should be examined. Typically, the thermocycler is programmed to produce the melting curve after the amplification. To do so, the temperature of the sample is augmented as the instrument continues to measure fluorescence. The double-stranded DNA denatures becoming single-stranded, and the dye, SYBR Green, dissociates and the emission of fluorescence stops. Additionally, the amplification efficiency can be determined from a series of dilutions originating a standard curve. The amplification efficacy is the most important indicator of the performance of a qPCR assay[116].

7. Statistical analysis

Statistical analysis was performed using GraphPad Prism and all data was expressed as mean ± standard deviation. A $p<0.05$ was considered statistically significant. Cell lines characterization based on gene expression was statistically analyzed by 1 way ANOVA followed by Tukey's multiple comparison test. Regarding metabolic activity, the half maximal inhibitory concentration (IC_{50}) was determined from log dose-response curves using non-linear regression analysis. In order to compare experimental data with controls and to examine the effect of PTL on metabolic activity and gene expression, analysis of variance using ANOVA or the non-parametrical equivalent (Kruskal-Wallis test) followed by Dunn's or Turkey's multiple comparison test was performed. Statistical analysis of PTL's effect on cell death, cell cycle, peroxide levels and $\Delta\Psi_M$ was performed using t-test or the non-parametrical equivalent (Mann-Whitney test).

Results

1. MM cell line characterization based on gene expression.

To assess if PTLs therapeutic targets are expressed in the cell lines utilized, the gene expression levels of the *REL*, *RELA*, *RELB*, *NFKB1*, and *IKBKB* genes were evaluated by RNA extraction followed by cDNA conversion and qPCR and the results are illustrated in Figure 8.

Concerning the expression levels of the five genes, no significant differences were detected between the cell lines. *REL* and *RELA* showed the higher expression values meanwhile *NFKB1* and *IKBKB* are expressed at a lower rate.

The *REL* expression levels were 1.78 in H929, 1.96 in H929-BTZ, 1.78 in H929-CFZ, and 2.14 in H929-IXZ. The *RELA* gene expression levels were 1.25, 1.06, 1.13, and 1.33 in H929, H929-BTZ, H929-CFZ, H929-IXZ respectively. The *NFKB1* gene expression was 0.77 in H929, 0.79 in H929-BTZ, 0.80 in H929-CFZ, 0.78 in H929-IXZ. Finally, the expression levels of *IKBKB* gene were 0.71, 0.67, 0.66 and 0.72 in H929, H929-BTZ, H929-CFZ, and H929-IXZ cell lines, respectively.

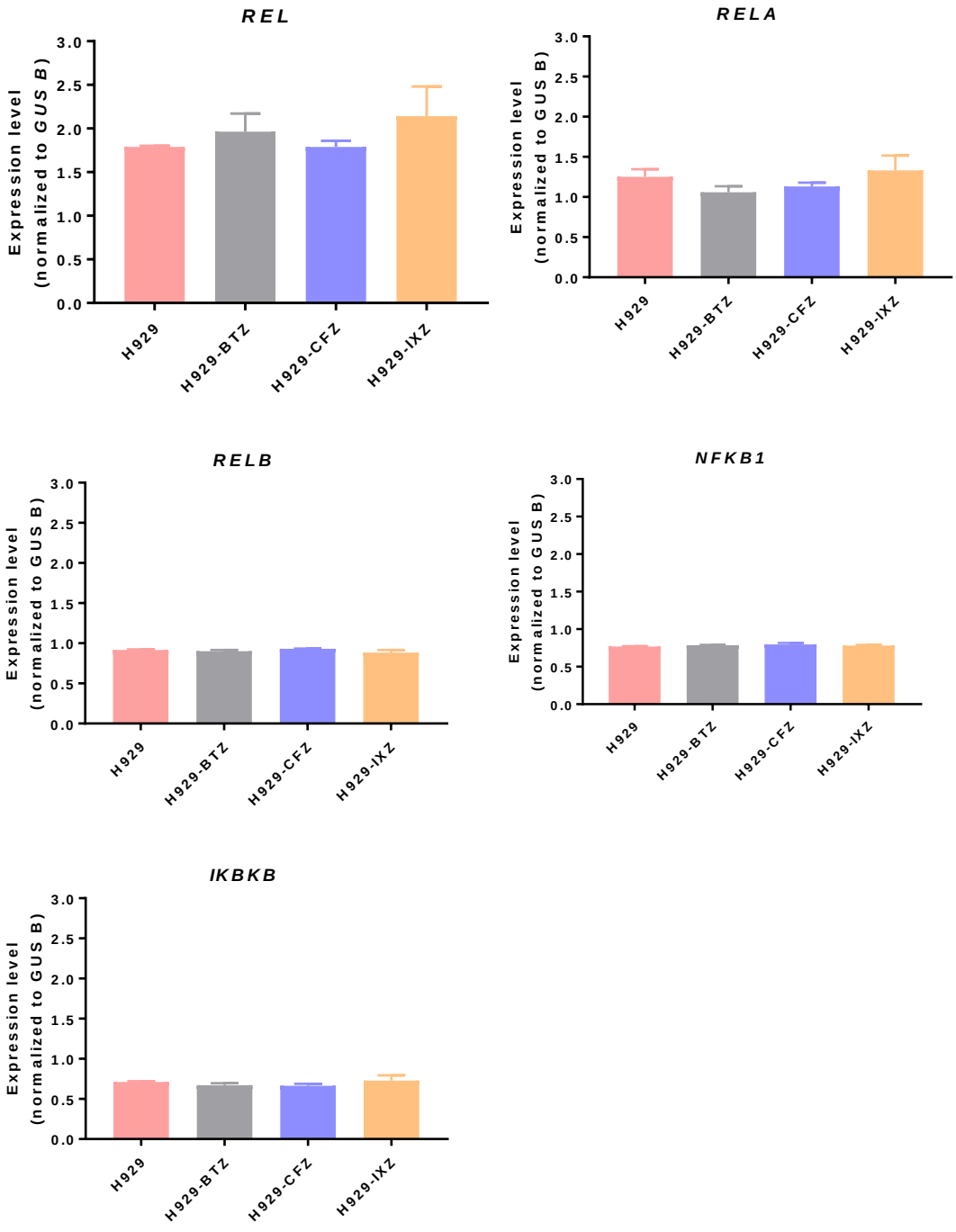

Figure 8- Expression of NF-κB pathway genes. The gene expression levels of the *REL*, *REL A*, *REL B*, *NFKB1*, and *IKBKB* genes were obtained by qPCR as described in the Materials and Methods section. The results represent the mean ± SEM of 3 independent experiences. A statistical analysis was performed using 1 way ANOVA followed by Tukey's multiple comparison test, in order to compare the expression in the resistant cell lines with the sensitive H929 cell line.

2. Cellular metabolic activity assessment.

The dose-response curves obtained with the resazurin assay are shown in Figure 9. By analyzing these curves, it is possible to conclude that PTL decreased the metabolic activity in both sensitive and resistant cell lines, in a time, dose and cell type dependent manner.

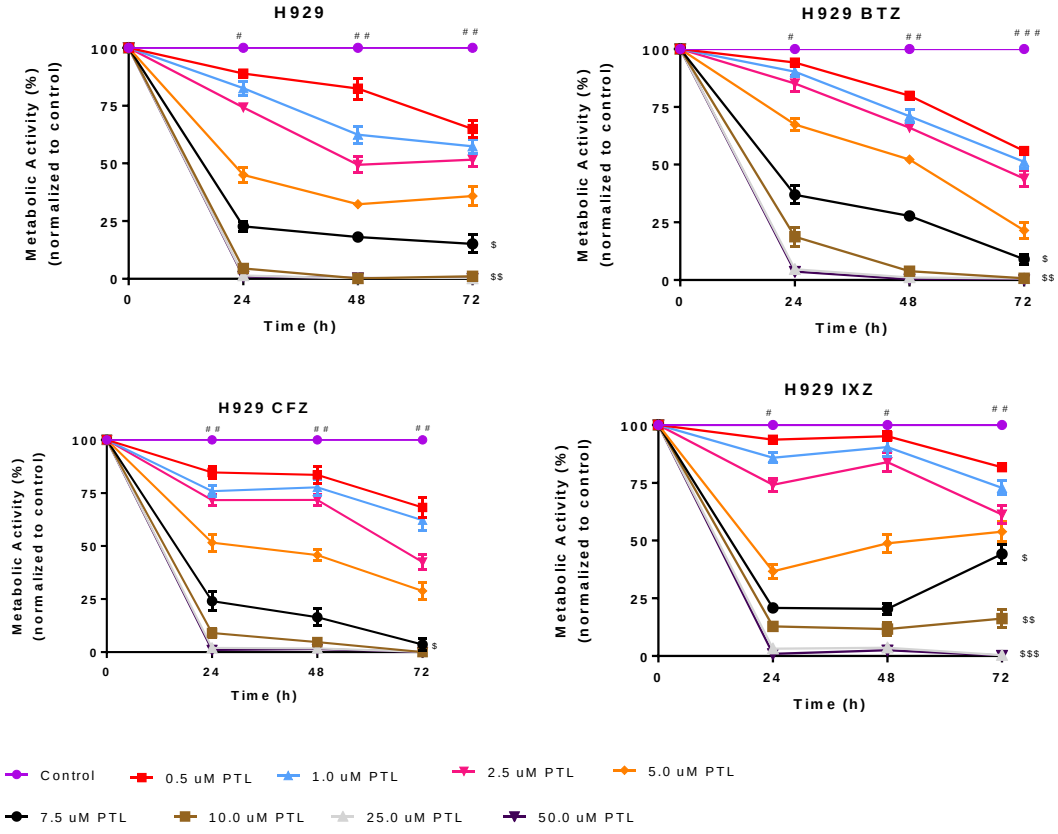

Figure 9- Dose-response curves of sensitive and resistant H929 cells. The metabolic activity was assessed by alamar blue assay in H929 cells and in their resistant counterparts H929-BTZ, H929-CFZ and H929-IXZ incubated in the absence and presence of 0.5, 1.0, 2.5, 5.0, 7.5, 10.0, 25.0, and 50.0 μM of PTL. Data is expressed in percentage of metabolic activity representing the mean ± SEM of 5 independent experiments. Statistical analysis was performed using Kruskal-Wallis test followed by Dunn's or Dunnett's multiple comparison test, being # p<0,05 comparing to 0 hours; ## p<0.01 comparing to 0 hours; ### p < 0.001 comparing to 0 hours; $ p<0.05, comparing to control; $$ p<0.01 comparing to control; $$$ p<0.001 comparing to control.

In H929 cells at 24 hours of incubation time, the three lower PTL concentrations (0.5, 1.0, and 2.5 μM) induced some decrease in the metabolic activity (11.08% loss of metabolic activity for 0.5 μM PTL, 17.46% loss of metabolic activity for 1.0 μM PTL, 24.78% loss of metabolic activity for 2.5 μM PTL). However, 5.0 μM PTL resulted in a decrease of 54.96%. In the four higher PTL concentrations (7.5, 10.0, 25.0, and 50.0 μM) the decrease was always superior to 75.00%. At 48 and 72 hours of incubation time, the PTL concentrations were able to produce a bigger effect on the reduction of metabolic activity. A similar pattern was observed in resistant cell lines. However, in H929-IXZ a reversal in the reduction of metabolic activity was observed for some concentrations after 24h of incubation.

On Table 1 are represented the PTL's IC_{50} values in the four cell lines, after 72 hours of incubation. One can conclude that the resistant cell line H929-IXZ is the one showing the higher IC_{50} value (7.32). This means that this cell line is the least susceptible to PTL. H929 and H929-CFZ showed similar IC_{50} values (2.41 and 2.37, respectively), whilst H929-BTZ revealed to be the most susceptible cell line to PTL (being 0.96 the IC_{50} value showed by this cell line).

Table 1- PTL's IC_{50} value in the four cell lines, after 72 hours of incubation with PTL.

Cell lines	IC_{50} 72H (μM)
H929	2.41
H929-BTZ	0.96
H929-CFZ	2.37
H929-IXZ	7.32

3. Cell death assessment.

Cell death was evaluated by FC. After a 72-hour incubation with PTL, the cells were stained using AV and 7-AAD. As observed in figure 10, the percentage of live cells decreased considerably in all cell lines: sensitive H929 showed a 14.50% decrease, H929-BTZ 16.25%, H929-CFZ 30.25%, and H929-IXZ 27.50%. PTL triggered a significant increase in the percentage cells in the late apoptosis/necrosis group in resistant cell lines (H929-BTZ showed a 12.00% increase, H929-CFZ showed a 19.75% increase, H929-IXZ showed a 20.00% increase). Moreover, in H929-CFZ it was also observed an increase (4.50%) in the percentage of early apoptotic cells. In the sensitive cell line, PTL caused an augmentation of 3.75% of cells in necrosis.

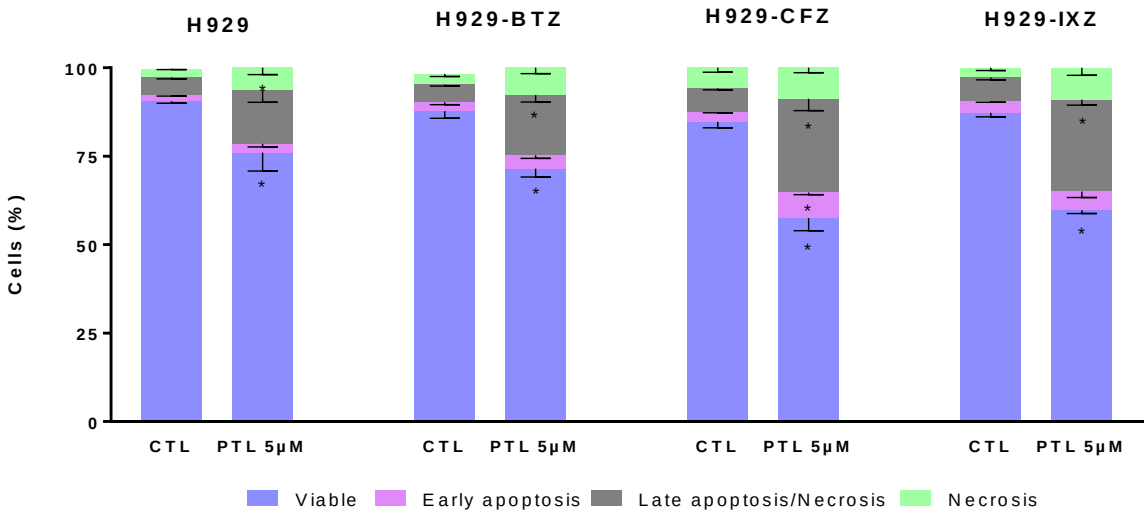

Figure 10- Cell death analysis of sensitive and resistant H929 cells. Cell death was evaluated in depth by FC using AV and 7-AAD double staining after a 72-hour incubation with PTL. Data is expressed in cellular percentage representing the mean ± SEM of 4 independent experiments. Statistical analysis was performed using a non-parametrical equivalent to a t-test (Mann-Whitney test), being * $p<0.05$, comparing to control.

In order to verify the morphological changes induced by PTL by optical mycroscopy, smears were stained by the May-Grunwald Giemsa protocol. In figure 11 it is possible to observe examples of the morphological characteristics observed. In fact, the cells exhibit lymphoblastic cellular characteristics as they look circular with a large

nucleus located eccentrically. There are morphological differences between the cells untreated and treated with PTL. The PTL brought up mainly typical apoptotic traits (such as shrinking of the cytoplasm and organelles, blebbing of the cellular membrane, and fragmentation of the cytoplasm into apoptotic bodies).

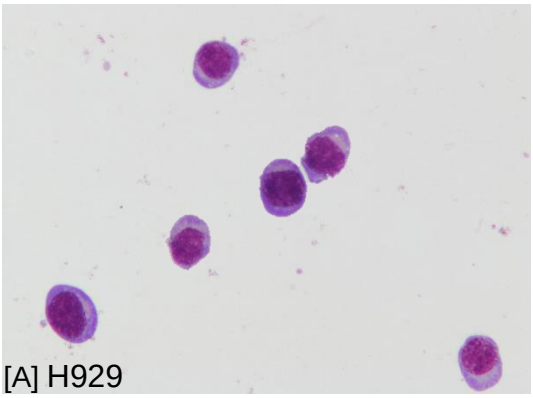

[A] H929

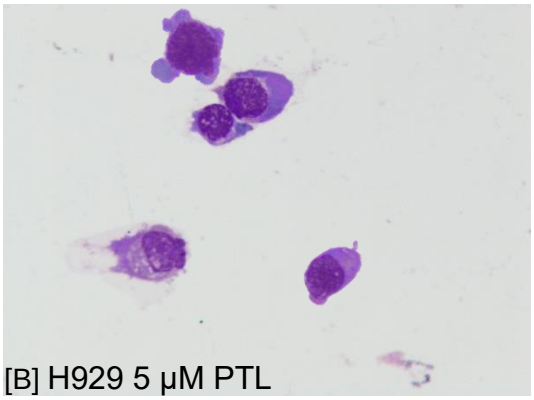

[B] H929 5 μM PTL

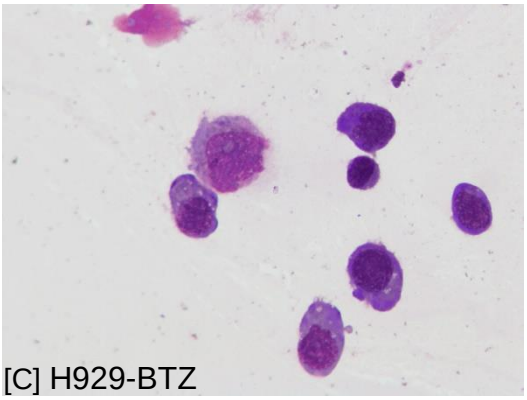

[C] H929-BTZ

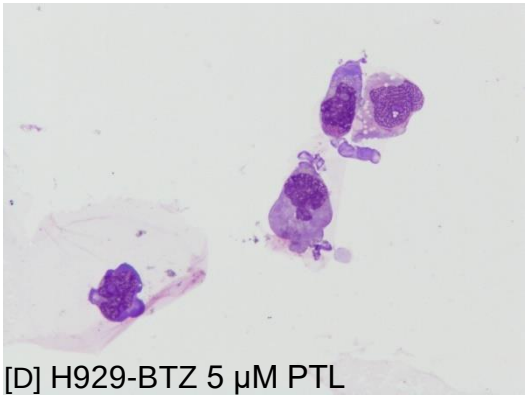

[D] H929-BTZ 5 μM PTL

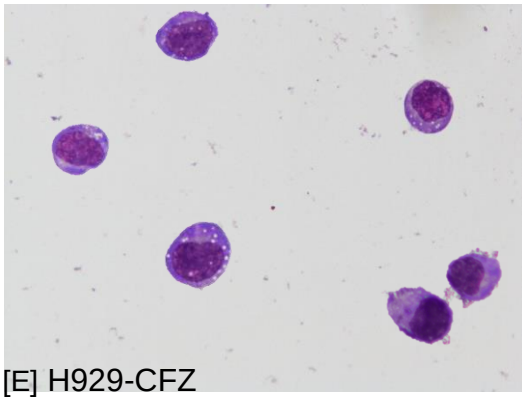

[E] H929-CFZ

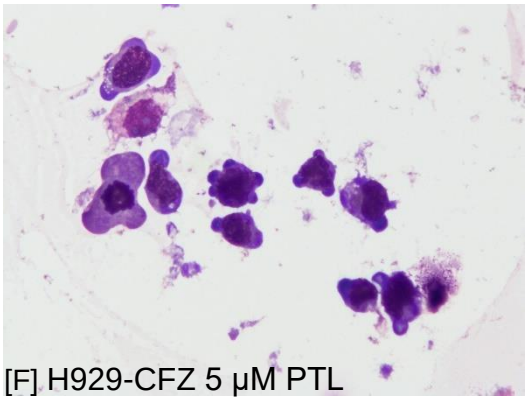

[F] H929-CFZ 5 μM PTL

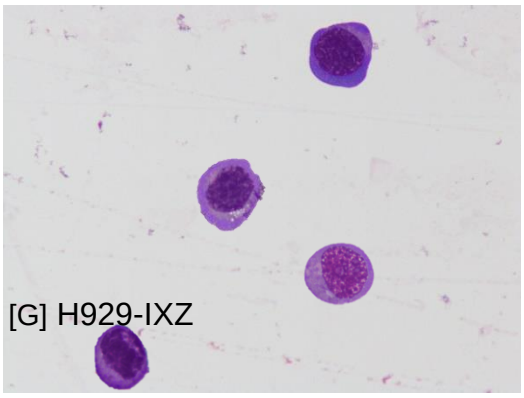

[G] H929-IXZ

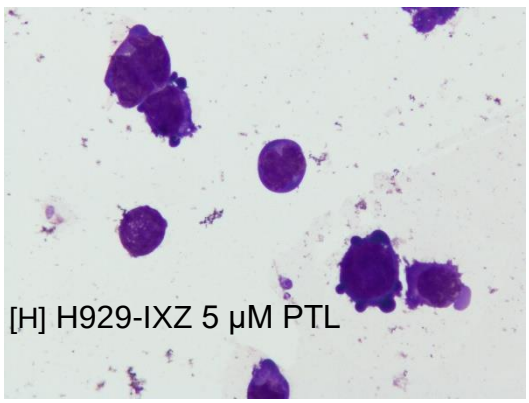

[H] H929-IXZ 5 μM PTL

Figure 11 – Morphlogical aspects of PI sensitive and resistant H929 cells lines treated (50X ampliation). Cells were incubated for 72 hours in absence or presence of different concentrations of PTL as described in the figure above. May-Grünwald-Giemsa staining was performed as described in the Materials and Methods section. The cells were analyzed by light microscopy.

4. Cell cycle assessment.

Cell cycle was evaluated by FC. After a 72-hour incubation without and with 5 μM of PTL, the cells were stained using propidium iodide/RNAse. The results are shown in table 2. Based on these results, PTL does not appear to have a cytostatic effect on any of the cell lines given that no statistically significant difference was found between the treated conditions and the controls. Particularly, the cell percentages of cells in the G0/G1, G2/M, and S did not alter substantially after the incubation with PTL.

Table 2- Cytostatic effect of PTL in MM cell lines sensitive and resistant to PI

		Sub G_0/G_1	G_0/G_1	S	G_2/M
H929	**CTL**	0.75 ± 0.22	66.75 ± 2.19	26.00 ± 1.80	7.25 ± 0.96
	5 μM PTL	1.50 ± 0.43	62.25 ± 2.13	30.00 ± 2.37	7.50 ± 0.83
H929-BTZ	**CTL**	1.00 ± 0.35	69.50 ± 2.14	22.00 ± 2.62	8.00 ± 0.79
	5 μM PTL	1.75 ± 0.96	65.75 ± 2.72	26.75 ± 3.78	6.00 ± 1.37
H929-CFZ	**CTL**	1.25 ± 0.54	63.75 ± 1.85	28.50 ± 1.25	8.00 ± 0.94
	5 μM PTL	3.50 ±1.35	60.75 ±3.90	33.25 ± 4.10	6.75 ± 0.22
H929-IXZ	**CTL**	2.75 ± 0.65	61.75 ± 4.46	32.00 ± 5.09	7.25 ± 1.24
	5 μM PTL	5.25 ± 0.96	61.50 ± 3.51	29.00 ± 2.67	9.50 ± 1.09

Data is expressed as percentage of cells in sub G_0/G_1 peak, G_0/G_1 phase, S phase, G_2/M phase and represent mean ± SEM obtained from 4 independent experiments. Statistical analyses were performed by comparison with control, using t-test.

5. Evaluation of oxidative stress and mitochondrial membrane potential

Oxidative stress has been correlated with some cellular events in cancer, such as cell proliferation, growth and death, in a concentration dependent manner. Moreover, the usage of PTL has been linked to an increase of intracellular ROS levels. Therefore, the levels of peroxides were assessed, by FC, using the $DCFH_2$-DA probe. Furthermore, the $\Delta\psi_M$ was also determined, using the JC-1 probe, by FC. In Table 3 are represented the peroxide levels and the M/A ratio in MM cell lines sensitive and resistant to PI.

PTL induced a significant increase on peroxides in both sensitive and resistant cell lines. H929-IXZ and H929-BTZ show the largest amount of intracellular peroxides [1.40-

fold in H929 (p=0.0013), 1.12-fold in H929-BTZ (p=0.0051), 1.14-fold in H929-CFZ (p=0.0125), and 1.32 in H929-IXZ (p=0.0002)].

Moreover, as mentioned before, the M/A ratio can translate the loss of $\Delta_{\Psi M}$ (since a high M/A ratio is indicative of a high loss of $\Delta_{\Psi M}$). Through the analysis of the results shown, all cell lines showed a significant increase of the M/A ratio after 72 hours of incubation with PTL [1.41-fold in H929 (p=0.0002), 1.82-fold in H929-BTZ (p=0.0002), 2.60-fold in H929-CFZ (p<0.0001), and 4.67 in H929-IXZ (p<0.0001)].

Table 3- Peroxide levels and ΔΨM in MM cell lines sensitive and resistant to PI.

		DCF	ΔΨM (M/A)
H929	**CTL**	331,00 ± 11,52	2,17 ± 0,05
	5 µM PTL	**464,00 ± 6,85****	**3,07 ± 0,03*****
H929-BTZ	**CTL**	442,00 ± 3,40	3,49 ± 0,06
	5 µM PTL	**494,00 ± 6,85****	**6,35 ± 0,09*****
H929-CFZ	**CTL**	389,33 ± 2,87	4,25 ± 0,04
	5 µM PTL	**444,00 ± 8,50***	**11,03 ± 0,14******
H929-IXZ	**CTL**	471,67 ± 3,07	3,20 ± 0,04
	5 µM PTL	**623,67 ± 8,82*****	**14,96 ± 0,40******

Data is expressed as mean ± SEM from 3 independent experiments. Statistical analyses were performed by comparing the treated condition with the control on each cell line, using t-test being * p<0.05, **p<0.01, *** p<0.001, and **** p<0.0001, comparing to control.

6. PTL's effect on gene expression

In order to verify if PTL's induced NF-κB inhibition caused alterations in gene expression, the genes *c-MYC* and *BCL-2* were assessed by RNA extraction followed by cDNA conversion and qPCR and the results are illustrated in Figure 12. *c-MYC* is a transcription factor that regulates many biological functions, including cell proliferation, cellular metabolism and apoptosis, whilst promoting the progression of MGUS to MM. A model proposed by Chesi, M. *et al* (2008) suggests that the MGUS to MM progression starts with the overexpression cyclin D gene as a result of a mutation (e.g. translocation, hyperdiploidy). Overexpression of Cyclin D in PCs allows them to bypass the early G_0/G_1 checkpoint, resulting in MGUS. One secondary event that alleviates the remaining cell cycle limitations is *c-MYC* overexpression. *c-MYC* has been shown to play a direct role in DNA replication while also controlling cell development towards S-phase[117]. *BCL-2* encodes for an anti-apoptotic protein that triggers MM cell survival and proliferation. Both of these genes are NF-κB target genes.

The *c-MYC* gene expression levels were very similar between the treated and the non-treated conditions and between the cell lines. No statistically significant difference was detected.

In regards of the *BCL-2* gene, even though no statistically significant difference was detected between the treated and the non-treated conditions and between the cell lines, a slight decrease seems to be induced by PTL, particularly in H929 and H929-IXZ (0.89-fold for H929 and 0.77-fold for H929-IXZ).

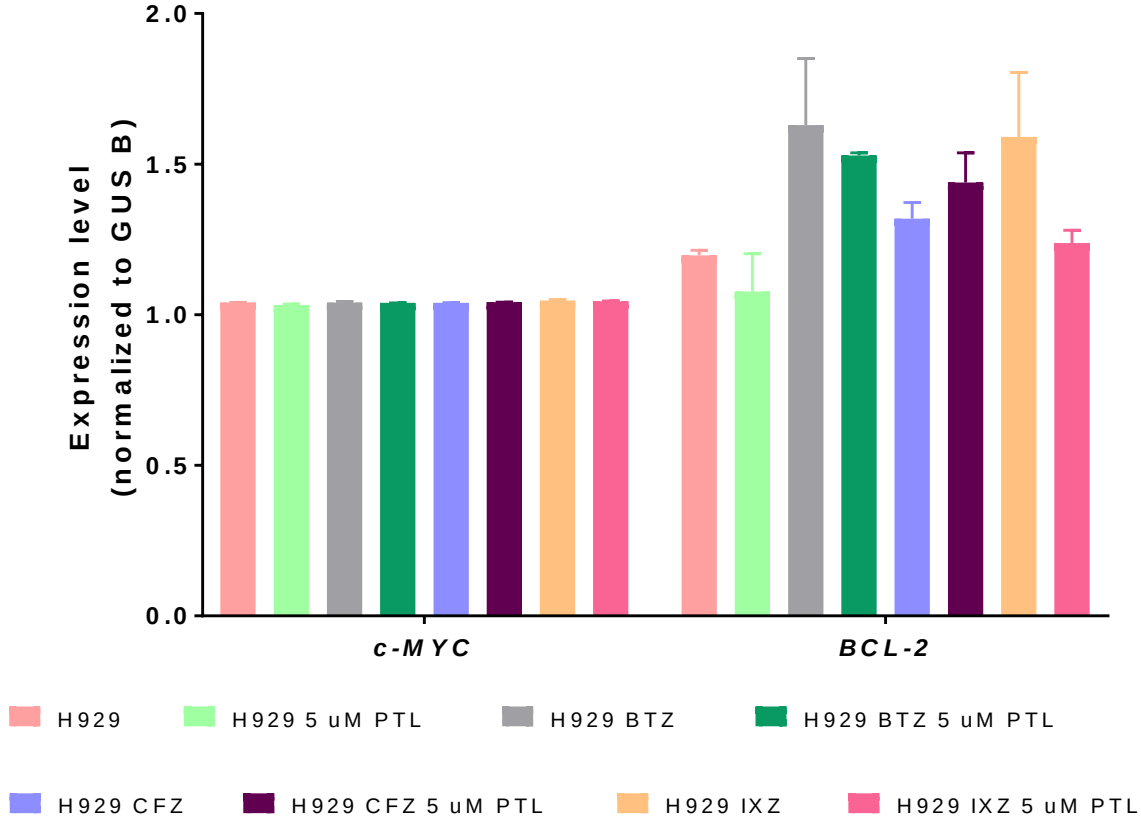

Figure 12 – *c-MYC* and *BCL-2 gene expression assessment.* The gene expression levels of the *c-MYC* and *BCL-2* genes were acquired through qPCR as described in the Materials and Methods section. The results represent the mean ± SEM of 3 independent experiences. A statistical analysis was performed using Kruskal-Wallis followed by Dunn's multiple comparison test, in order to compare the expression in the resistant cell lines with the sensitive H929 cell line.

Discussion

1. Evaluation of the therapeutic potential of PTL in MM

Therapeutic agents such as PIs, IMiDs, and MoAbs, have significantly improved MM patients' quality of life. However, this disease remains incurable due to drug resistance, therapeutic failure, and eventual illness relapse. Drug resistance can be caused by genetic and epigenetic alterations, atypical drug transport and metabolism, dysregulation of apoptosis, activation of autophagy, persistence of drug-resistant CSCs, or a dysfunctional tumor microenvironment. On another hand, a frequent event in MM is the activation of NF-κB, commonly known for its anti-apoptotic effects promoting cancer cell survival and the expression of antiapoptotic genes. PTL is a potent antineoplastic drug that inhibits the NF-κB factor. In this context, the aim of this project was to assess the capacity of PTL in overcoming MM's resistance to proteosome inhibitors BTZ, CFZ and IXZ.

Primarily, the gene expression levels of the *REL*, *RELA*, *RELB*, *NFKB1*, and *IKBKB* genes were evaluated by qPCR in order to assess if PTLs therapeutic targets are expressed in the cell lines utilized. These genes are involved in the NF-κB pathway coding for the proteins c-REL, p65, REL B, p105 and IKKβ, respectively. The results showed that *RELA*, *RELB* and *c-REL* are expressed at a very high level in all the cell lines equally. Hence, this outcome was not surprising since the NF-κB factor is highly expressed in MM cells[45].

Nevertheless, the evaluation of the *NFKB1* and *IKBKB* genes demonstrated that these genes are expressed at a lower level. As the NF-κB pathway is constitutively expressed in MM cells, it was expected for the *NFKB1* gene to have a higher expression. The *IKBKB* gene encodes for the IKKβ protein that targets IκBα for degradation by the proteosome, leading to NF-κB activation[39]. However, the IKKβ protein is not the only player in IκB's inhibition. In fact, NEMO and IKKα are also crucial for canonical and non-canonical NF-κB activation[28], so the confluence of the expression levels of these factors will dictate the activation of NF-κB. The activation of the classical NF-κB pathway favors the formation of p65/p50 and c-Rel/p50 heterodimers, leading to the overexpression of the *RELA*, *REL* and *NFKB1* genes. Contrarily, the activation of the non-canonical NF-κB pathway, favors the formation of Rel B/p52 heterodimers, leading to the overexpression of *RELB*[118].Even though the *RELA* gene was substantial expressed, the lower *NFKB1* and *IKBKB* expression can signify that the non-canonical NF-κB pathway is being activated facilitating the formation of Rel B/p52 heterodimers.

As PTLs targets were proven to be expressed in the MM, PTL could be a potential agent to tackle the cancer cells. The cell lines were then incubated with PTL, in order to

assess their metabolic activity. In the results, it was noted that PTL exerted a time and dose dependent reduction on the metabolic activity of the cell lines. In fact, at 72 hours the lowest value of metabolic activity was obtained in most of the tested conditions in most of the cell types.

Moreover, it was confirmed that the resistant H929-IXZ cell line is less susceptible to PTL than the sensitive cell line. In fact, after 72 hours of incubation, it showed the higher IC_{50}.

As a matter of fact, the resistant cell lines can exhibit MDR resulting in a low cellular capacity to accumulate drugs[74]. As stated earlier, the MDR mechanism can be caused by the overexpression of certain members of the ABC transporter family of proteins, like the transporters Pgp/ABCB1 and ABCC1. These membrane proteins are able to export a wide range of molecules, including PTL, across cellular membranes leading to a reduction in intracellular drug concentrations[51,75,119]. Additionally it has been previously described in a study performed in the FMUC Laboratory of Oncobiology and Hematology, that these membrane transporters are overexpressed in MM resistant cells[120]. Therefore, the drug resistance originally established in the resistant cell lines to the drugs BTZ, CFZ and IXZ can now be instigating cell resilience towards PTL via MDR.

A drug can cause cellular metabolic activity diminution by exerting a cytotoxic and/or cytostatic activity. Hence, it was necessary to assess if this decline was due to cell death or to an arrest in cellular proliferation. For the purpose of assessing on cell death, FC assays were executed using the AV/7-AAD double staining. The percentage of live, early apoptotic, late apoptotic/necrotic and necrotic cells was estimated (live cells were not marked with any of the molecules, early apoptotic cells were marked with AV, late apoptotic/necrotic cells were marked with both of the molecules and necrotic cells were stained with 7-AAD).

PTL induced cancer cell death mostly by apoptosis which corroborates with the existing literature[121,122,123]. Furthermore, PTL has been proven to be effective not only against MM but also towards other types of malignant illnesses[124,125,126,127,128].

Moreover, apoptosis causes morphological cellular alterations like condensation of chromatin, cleavage of nuclear DNA, shrinking of the cytoplasm and organelles, blebbing of the cellular membrane, and fragmentation of the cytoplasm into apoptotic bodies. In order to verify if PTL caused structural changes in the cells, morphological studies were conducted by implementing the May-Grünwald Giemsa smear staining protocol. In fact, PTL promoted mainly typical apoptotic attributes.

To assess if PTL might reduce cellular metabolic activity through cytostatic activity, FC assays were completed using propidium iodide/RNAse solution. No major difference was found between the non-treated and the treated conditions. A study by Suvannasankha *et al.* (2008) also reached the same conclusion[121]. In MM cells, the incubation with PTL is preceded by immediate activation of apoptosis, which leaves no time period for significant cell cycle alteration.

However PTL has been proven to cause cell cycle arrest in G_0/G_1 phase in bladder[124], skin[129], gastric[126] cancer as well as in chronic myeloid leukemia[130]. Also, PTL caused an arrest in the G_2/M phase in glioblastoma[131] and in breast cancer[125].

Consequently, one can conclude that PTL reduces cell metabolic activity through its cytotoxic effects (leading to cell death) and that this compound showed no cytostatic action.

Consequently, one can conclude that PTL reduces cell metabolic activity through its cytotoxic effects (leading to cell death) and that this compound showed no cytostatic action in the MM cell lines studied.

Incubation with PTL has also been linked to an increase of intracellular ROS levels and a decrease in antioxidant defenses, leading to oxidative stress. Moreover, oxidative stress has been correlated with some cellular events in cancer, such as cell proliferation, growth and death. Dysregulation of different aspects of antioxidant defense, including as the thioredoxin system, glutaredoxin system and catalase, is involved in the cytotoxicity mechanisms of ROS-inducing substances. In fact, auranofin, arsenic trioxide, and disulfiram, are FDA-approved therapeutic alternatives for other types of cancers, are currently being studied to see if they may be used to treat MM[132]. Auranofin has been found to block thioredoxin-mediated redox signaling and reduce MM cell proliferation[133].

Therefore, to evaluate the oxidative stress of MM cell lines, basal levels peroxides were assessed, by FC, using the $DCFH_2$-DA probe. The results confirmed that PTL increased peroxide quantities in all of the cell lines, particularly in the resistant ones. H929-IXZ and H929-BTZ showed the largest amount of intracellular peroxides.

H929-BTZ, H929-CFZ, and H929-IXZ are resistant to the proteosome inhibitors BTZ, CFZ, and IXZ, respectively. The inhibition of proteasomes leads to unfolded protein buildup, triggering ER stress[134]. On another hand, a known side effect of ER stress is oxidative stress[135]. Due to a greater burden of unfolded proteins during ER stress, the activity of some enzymes increases, resulting in higher levels of ROS. Protein disulfide

isomerase, endoplasmic reticulum oxidoreductin, NADPH oxidase complexes, and mitochondrial electron transport enzymes are amongst the enzymatic components implicated in ER stress-dependent ROS generation[136,137]. The production of oxidative stress is only partially facilitated by ROS generated as a consequence of protein folding[136]. Another key component of ROS formation is the mechanism involved in calcium homeostasis. Ca^{2+} leaking from the ER into the cytosol might thereby cause oxidative stress[138]. These facts elucidate the reason behind the higher peroxide levels that were obtained in the H929-BTZ and on H929-IXZ cell lines.

Furthermore, the $\Delta\psi_M$ was also determined, using the JC-1 probe, by FC. The M/A ratio reveals the $\Delta\psi_M$, being that a higher M/A ratio is associated with a greater loss of $\Delta\psi_M$. Through the analysis of the results regarding the $\Delta\psi_M$, it is possible to conclude that in all cell lines, a significant decrease of $\Delta\psi_M$ was observed. Especially, the biggest $\Delta\psi_M$ loss was noted in H929-IXZ, followed by H929-CFZ.

As mentioned before, the resistant cell lines displayed the higher ROS levels. ROS activate many enzymatic cascades and transcription factors, which play a vital role in physiological cellular activities. Excessive ROS values are often harmful causing mitochondrial depolarization, cytochrome c release, lipid peroxidation, and DNA damage[139]. Consequently, finding the higher loss of $\Delta\psi_M$ on a resistant cell line was not surprising. The fact that PTL leads to mitochondria disturbance is in agreement with studies performed in MM[121], acute myeloblastic leukemia[140], hepatocellular carcinoma[141], but also in lung[127], ovarian[142], and breast[128] cancer.

The results obtained in the cell death evaluation assays are consistent with the JC-1 results since the H929-IXZ cell line showed both the biggest $\Delta\psi_M$ loss and the highest increase in the percentage of cells in the late apoptosis/necrosis. In fact, after mitochondrial membrane depolarization, the pro-apoptotic molecule cytochrome c causes the initiation of caspase-9, that sequentially activates caspase-3 and 7 giving rise to apoptosis[143].

The NF-κB pathway is responsible for regulating the expression of many genes, including *c-MYC* and *BCL-2* neoplastic genes. Thus, PTL's inhibition of NF-κB can affect the expression of these genes. For the purpose of evaluating PTL's effect on gene expression, *c-MYC* and *BCL-2* expression levels were assessed by qPCR.

Concerning *c-MYC* gene, the results showed a homogenous value of expression amongst all conditions of all the cell lines. This fact shows that *c-MYC* does not have its expression reliant on NF-κB, thus it is not affected by NF-κB inhibition by PTL. In fact,

the gene is originally expressed in the transition from MGUS to MM, maintaining its high expression levels in the malignant stage of the disease[144]. However, the down regulation of *c-MYC* by PTL was noted in a study executed on a non-small cell lung cancer cell line[145]. Moreover, *c-MYC* expression levels can be strongly associated with cell proliferation. In fact, the fist described *c-MYC* target genes (such as cyclins) are in fact regulators of cell cycle. As *c-MYC* stimulates cell cycle progression and that the expression levels of this gene were not affected by PTL, this might help explain why no changes were noted in the cell cycle[146].

As mentioned before, *BCL-2* expression can also be triggered by NF-κB[147]. According to the statement that the NF-κB factor is highly expressed in MM cell lines[18], it was expected high *BCL-2* expression values in the non-treated conditions, which was observed. On the same note, the incubation with PTL was anticipated to reduce *BCL-2* expression values, because of the PTL's inhibition of NF-κB. Even though, no statistically significant alteration was observed, a decrease in *BCL-2* gene expression levels was noted in the PTL treated condition. Additionally, *BCL-2* overexpression is triggered not only by the NF-κB factor but also by genetic mutations, such as translocations involving the IgH locus[148]. The down regulation of *BCL-2* by PTL was also noted in a study executed on cervical and breast cancer cell lines[128] and in one study performed in pancreatic cancer cells[149]. *BCL-2* binds to pro-apoptotic members such as BAX, preventing loss of $\Delta\psi_M$ and cytochrome c release. PTL's induced reduction of *BCL-2* gene expression levels, accompanied by high levels of BAX, culminates in cell death[150]. Also, a *in vivo* study noted that PTL decreased the BCL-2 and BCL-XL protein levels, whilst increasing BAX protein levels leading to apoptosis through mitochondrial failure[151].

Conclusion

The present study was able to elucidate on the effects of PTL in MM cells resistant to PIs, in order to complement the knowledge on this research area. The main conclusions are the following:

1. Gene expression appraisal results showed that *RELA*, *RELB*, and *c-REL* are expressed at a very high level in all the cell lines, whilst *NFKB1* and *IKBKB* were expressed at a lower rate.

2. PTL caused a time, cell and dose dependent decline on the metabolic activity. The biggest drop in metabolic activity was obtained at 72 hours. Moreover, it was confirmed that the resistant cell line H929- IXZ is less vulnerable to PTL than the sensitive cell line.

3. Cell death evaluation by CF assays, showed that PTL sparked a significant increase in the cellular percentage in the late apoptotic/necrotic group in resistant cell lines and a rise of the cell percentage in the early apoptotic group in H929-CFZ.

4. Cell cycle evaluation revealed no major differences between the treated conditions and the control.

5. PTL treated cells showed higher levels of ROS and a loss of $\Delta\psi_M$.

6. Significant changes in the expression of *BCL-2* and *c-MYC* were not exhibited, neither between the treated conditions and the control or between the cells lines.

This project discloses that PTL is capable of circumventing drug resistance to PI, being quite useful at inducing cell death. As future perspectives, it would be relevant to characterize the cell lines on their expression of *NFKB2*. Also, it would be interesting to evaluate the effect of PTL on other genes such as *STAT3*, since this compound is an effective inhibitor of STAT proteins. Additionally, it would be interesting to assess PTL's effect on epigenetic factors (like DNMT1, DNMT3b and HDAC1). Moreover, the cell cycle regulating gene, *CCND1,* and the antiapoptotic genes *XIAP* and *BIRC5,* would be appropriate to evaluate as they represent important MM molecular therapeutic targets. Also, it would be pertinent to conduct association assays between PTL and the three PIs to verify if this compound can re-sensitize the resistant cells to PIs.

References

1. Ho, M. S. H., Medcalf, R. L., Livesey, S. A. & Traianedes, K. The dynamics of adult haematopoiesis in the bone and bone marrow environment. *Br. J. Haematol.* **170**, 472–486 (2015).

2. Orkin, S. H. & Zon, L. I. Hematopoiesis: an evolving paradigm for stem cell biology. *Cell* **132**, 631–644 (2008).

3. Rocamonde, B., Carcone, A., Mahieux, R. & Dutartre, H. HTLV-1 infection of myeloid cells: from transmission to immune alterations. *Retrovirology* **16**, 45 (2019).

4. Wadhwa, M. & Thorpe, R. Haematopoietic growth factors and their therapeutic use. *Thromb. Haemost.* **99**, 863–873 (2008).

5. De, S. & Barnes, B. J. B cell transcription factors: Potential new therapeutic targets for SLE. *Clin. Immunol.* **152**, 140–151 (2014).

6. Hoffbrand, A. V. & Paul A. H. Moss. *Hoffbrand's Essential Haematology*. (Wiley-Blackwell, 2016).

7. Hystad, M. E. *et al.* Characterization of early stages of human B cell development by gene expression profiling. *J. Immunol.* **179**, 3662–3671 (2007).

8. Kumar, S. K. *et al.* Multiple myeloma. *Nat. Rev. Dis. Prim.* **3**, 17046 (2017).

9. Pinto, V. *et al.* Multiple myeloma: Available therapies and causes of drug resistance. *Cancers (Basel).* **12**, 1–32 (2020).

10. Ludwig, H., Novis Durie, S., Meckl, A., Hinke, A. & Durie, B. Multiple Myeloma Incidence and Mortality Around the Globe; Interrelations Between Health Access and Quality, Economic Resources, and Patient Empowerment. *Oncologist* **25**, e1406–e1413 (2020).

11. Waxman, A. J. *et al.* Racial disparities in incidence and outcome in multiple myeloma: a population-based study. *Blood* **116**, 5501–5506 (2010).

12. Rajkumar, S. V. *et al.* International Myeloma Working Group updated criteria for the diagnosis of multiple myeloma. *Lancet Oncol.* **15**, e538–e548 (2014).

13. Nakaya, A. *et al.* Impact of CRAB symptoms in survival of patients with symptomatic myeloma in novel agent era. **9**, (2017).

14. Rajkumar, S. V. Multiple myeloma: 2020 update on diagnosis, risk-stratification and management. *Am. J. Hematol.* **95**, 548–567 (2020).

15. Jennifer L. J. Heaney *et al.* Excluding myeloma diagnosis using revised thresholds for serum free light chain ratios and M-protein levels. *Haematologica* **105**, e169–e171 (2020).

16. Ben-Neriah, Y. & Karin, M. Inflammation meets cancer, with NF-κB as the matchmaker. *Nat. Immunol.* **12**, 715–723 (2011).

17. Wardyn, J. D., Ponsford, A. H. & Sanderson, C. M. Dissecting molecular cross-talk

between Nrf2 and NF-κB response pathways. *Biochem. Soc. Trans.* **43**, 621–626 (2015).

18. Nagel, D., Vincendeau, M., Eitelhuber, A. C. & Krappmann, D. Mechanisms and consequences of constitutive NF-κB activation in B-cell lymphoid malignancies. *Oncogene* **33**, 5655–5665 (2014).

19. Chen, D., Frezza, M., Schmitt, S., Kanwar, J. & P. Dou, Q. Bortezomib as the First Proteasome Inhibitor Anticancer Drug: Current Status and Future Perspectives. *Curr. Cancer Drug Targets* **11**, 239–253 (2011).

20. Taniguchi, K. N-κB, inflammation, immunity and cancer: coming of age. *Nat. Rev. Immunol.* **18 (5)**, 309–324 (2018).

21. Giuliani, C., Bucci, I. & Napolitano, G. The Role of the Transcription Factor Nuclear Factor-kappa B in Thyroid Autoimmunity and Cancer . *Frontiers in Endocrinology* vol. 9 471 (2018).

22. Mitchell, S., Vargas, J. & Hoffmann, A. Signaling via the NFκB system. *WIREs Syst. Biol. Med.* **8**, 227–241 (2016).

23. Roy, P., Sarkar, U. A. & Basak, S. The NF-κB Activating Pathways in Multiple Myeloma. *Biomedicines* **6**, 59 (2018).

24. Jovanović, K. K. *et al.* Targeting MYC in multiple myeloma. *Leukemia* **32**, 1295–1306 (2018).

25. Xiao, G. & Fu, J. NF-κB and cancer: a paradigm of Yin-Yang. *Am. J. Cancer Res.* **1**, 192–221 (2011).

26. Jost, P. J. & Ruland, J. Aberrant NF-kappaB signaling in lymphoma: mechanisms, consequences, and therapeutic implications. *Blood* **109**, 2700–2707 (2007).

27. Sun, S.-C. Non-canonical NF-κB signaling pathway. *Cell Res.* **21**, 71–85 (2011).

28. Sun, X.-F. & Zhang, H. NFKB and NFKBI polymorphisms in relation to susceptibility of tumour and other diseases. *Histol. Histopathol.* **22**, 1387–1398 (2007).

29. Rayet, B. & Gélinas, C. Aberrant rel/nfkb genes and activity in human cancer. *Oncogene* **18**, 6938–6947 (1999).

30. Lin, L., DeMartino, G. N. & Greene, W. C. Cotranslational biogenesis of NF-kappaB p50 by the 26S proteasome. *Cell* **92**, 819–828 (1998).

31. Yu, Y., Wan, Y. & Huang, C. The biological functions of NF-kappaB1 (p50) and its potential as an anti-cancer target. *Curr. Cancer Drug Targets* **9**, 566–571 (2009).

32. Xiao, G., Harhaj, E. W. & Sun, S. C. NF-kappaB-inducing kinase regulates the processing of NF-kappaB2 p100. *Mol. Cell* **7**, 401–409 (2001).

33. Rao, P. H. *et al.* Chromosomal and Gene Amplification in Diffuse Large B-Cell Lymphoma. *Blood* **92**, 234–240 (1998).

34. Gilmore, T. D. & Gerondakis, S. The c-Rel Transcription Factor in Development and Disease. *Genes Cancer* **2**, 695–711 (2011).

35. Mathew, S., Murty, V. V, Dalla-Favera, R. & Chaganti, R. S. Chromosomal localization of genes encoding the transcription factors, c-rel, NF-kappa Bp50, NF-kappa Bp65, and lyt-10 by fluorescence in situ hybridization. *Oncogene* **8**, 191–193 (1993).

36. Bours, V., Azarenko, V., Dejardin, E. & Siebenlist, U. Human RelB (I-Rel) functions as a kappa B site-dependent transactivating member of the family of Rel-related proteins. *Oncogene* **9**, 1699–1702 (1994).

37. Kaltschmidt, B., Greiner, J. F. W., Kadhim, H. M. & Kaltschmidt, C. Subunit-Specific Role of NF-κB in Cancer. *Biomedicines* **6**, (2018).

38. Weih, F. *et al.* Multiorgan inflammation and hematopoietic abnormalities in mice with a targeted disruption of RelB, a member of the NF-kappa B/Rel family. *Cell* **80**, 331–340 (1995).

39. Kai, X. *et al.* IκB Kinase β (IKBKB) Mutations in Lymphomas That Constitutively Activate Canonical Nuclear Factor κB (NFκB) Signaling. *J. Biol. Chem.* **289**, 26960–26972 (2014).

40. Chapman, M. A. *et al.* Initial genome sequencing and analysis of multiple myeloma. *Nature* **471**, 467–472 (2011).

41. Annunziata, C. M. *et al.* Frequent engagement of the classical and alternative NF-kappaB pathways by diverse genetic abnormalities in multiple myeloma. *Cancer Cell* **12**, 115–130 (2007).

42. Trompouki, E. *et al.* CYLD is a deubiquitinating enzyme that negatively regulates NF-kappaB activation by TNFR family members. *Nature* **424**, 793–796 (2003).

43. Kovalenko, A. *et al.* The tumour suppressor CYLD negatively regulates NF-kappaB signalling by deubiquitination. *Nature* **424**, 801–805 (2003).

44. Demchenko, Y. N. *et al.* Classical and/or alternative NF-kappaB pathway activation in multiple myeloma. *Blood* **115**, 3541–3552 (2010).

45. Keats, J. J. *et al.* Promiscuous mutations activate the noncanonical NF-kappaB pathway in multiple myeloma. *Cancer Cell* **12**, 131–144 (2007).

46. Debes-Marun, C. S. *et al.* Chromosome abnormalities clustering and its implications for pathogenesis and prognosis in myeloma. *Leukemia* **17**, 427–436 (2003).

47. Varfolomeev, E. *et al.* Cellular Inhibitors of Apoptosis Are Global Regulators of NF-κB and MAPK Activation by Members of the TNF Family of Receptors. *Sci. Signal.* **5**, ra22 LP-ra22 (2012).

48. Odqvist, L. *et al.* NIK controls classical and alternative NF-κB activation and is necessary for the survival of human T-cell lymphoma cells. *Clin. cancer Res. an Off. J. Am. Assoc. Cancer Res.* **19**, 2319–2330 (2013).

49. Chen, D. & Dou, Q. P. The ubiquitin-proteasome system as a prospective molecular target for cancer treatment and prevention. *Curr. Protein Pept. Sci.* **11**, 459–470 (2010).

50. Niewerth, D. *et al.* Molecular basis of resistance to proteasome inhibitors in hematological malignancies. *Drug Resist. Updat. Rev. Comment. Antimicrob. Anticancer Chemother.* **18**, 18–35 (2015).

51. Bai, Y. & Su, X. Updates to the drug-resistant mechanism of proteasome inhibitors in multiple myeloma. *Asia. Pac. J. Clin. Oncol.* **17**, 29–35 (2021).

52. Ito, S. Proteasome Inhibitors for the Treatment of Multiple Myeloma. *Cancers (Basel).* **12**, 265 (2020).

53. Kumar, S. *et al.* Randomized, multicenter, phase 2 study (EVOLUTION) of combinations of bortezomib, dexamethasone, cyclophosphamide, and lenalidomide in previously untreated multiple myeloma. *Blood* **119**, 4375–4382 (2012).

54. Cavo, M. *et al.* Role of consolidation therapy in transplant eligible multiple myeloma patients. *Semin. Oncol.* **40**, 610–617 (2013).

55. Derudas, D., Capraro, F., Martinelli, G. & Cerchione, C. How I manage frontline transplant-ineligible multiple myeloma. *Hematol. Rep.* **12**, 8956 (2020).

56. Kane, R. C., Farrell, A. T., Sridhara, R. & Pazdur, R. United States Food and Drug Administration approval summary: bortezomib for the treatment of progressive multiple myeloma after one prior therapy. *Clin. cancer Res. an Off. J. Am. Assoc. Cancer Res.* **12**, 2955–2960 (2006).

57. Hideshima, T. *et al.* Bortezomib induces canonical nuclear factor-kappaB activation in multiple myeloma cells. *Blood* **114**, 1046–1052 (2009).

58. Corso, A. *et al.* Bortezomib plus dexamethasone can improve stem cell collection and overcome the need for additional chemotherapy before autologous transplant in patients with myeloma. *Leuk. Lymphoma* **51**, 236–242 (2010).

59. Jagannath, S. *et al.* Extended follow-up of a phase 2 trial of bortezomib alone and in combination with dexamethasone for the frontline treatment of multiple myeloma. *Br. J. Haematol.* **146**, 619–626 (2009).

60. Harousseau, J.-L. *et al.* Bortezomib plus dexamethasone as induction treatment prior to autologous stem cell transplantation in patients with newly diagnosed multiple myeloma: results of an IFM phase II study. *Haematologica* **91**, 1498–1505 (2006).

61. Herndon, T. M. *et al.* U.S. Food and Drug Administration Approval: Carfilzomib for the Treatment of Multiple Myeloma. *Clin. Cancer Res.* **19**, 4559 LP – 4563 (2013).

62. Siegel, D. S. *et al.* A phase 2 study of single-agent carfilzomib (PX-171-003-A1) in

patients with relapsed and refractory multiple myeloma. *Blood* **120**, 2817–2825 (2012).

63. A. Keith Stewart, M.B., Ch.B., S. Vincent Rajkumar, M.D., Meletios A. Dimopoulos, M. D. *et al.* Carfilzomib, Lenalidomide, and Dexamethasone for Relapsed Multiple Myeloma. (2015) doi:10.1056/NEJMoa1411321.

64. Efentakis, P. *et al.* Molecular mechanisms of carfilzomib-induced cardiotoxicity in mice and the emerging cardioprotective role of metformin. *Blood* **133**, 710–723 (2019).

65. Shirley, M. Ixazomib: First Global Approval. *Drugs* **76**, 405–411 (2016).

66. Hungria, V. T. de M. *et al.* New proteasome inhibitors in the treatment of multiple myeloma. *Hematol. Transfus. cell Ther.* **41**, 76–83 (2019).

67. Moreau, P. *et al.* Oral Ixazomib, Lenalidomide, and Dexamethasone for Multiple Myeloma. *N. Engl. J. Med.* **374**, 1621–1634 (2016).

68. Kumar, S. K. *et al.* Safety and tolerability of ixazomib , an oral proteasome inhibitor , in combination with lenalidomide and dexamethasone in patients with previously untreated multiple myeloma : an open-label phase 1 / 2 study. *Lancet Oncol.* **15**, 1503–1512 (2014).

69. Nijhof, I. S., Donk, N. W. C. J. Van De & Zweegman, S. Current and New Therapeutic Strategies for Relapsed and Refractory Multiple Myeloma : An Update. *Drugs* **78**, 19–37 (2018).

70. Mogollón, P. *et al.* Biological Background of Resistance to Current Standards of Care in Multiple Myeloma. *Cells* vol. 8 (2019).

71. Robak, P., Drozdz, I., Szemraj, J. & Robak, T. Drug resistance in multiple myeloma. *Cancer Treat. Rev.* **70**, 199–208 (2018).

72. D'Agostino, M., Bertamini, L., Oliva, S., Boccadoro, M. & Gay, F. Pursuing a Curative Approach in Multiple Myeloma: A Review of New Therapeutic Strategies. *Cancers (Basel).* **11**, (2019).

73. Robak, P., Drozdz, I., Szemraj, J. & Robak, T. Drug resistance in multiple myeloma. *Cancer Treat. Rev.* **70**, 199–208 (2018).

74. Narayanan, S. *et al.* Targeting the ubiquitin-proteasome pathway to overcome anti-cancer drug resistance. *Drug Resist. Updat. Rev. Comment. Antimicrob. Anticancer Chemother.* **48**, 100663 (2020).

75. Sun, Y.-L., Patel, A., Kumar, P. & Chen, Z.-S. Role of ABC transporters in cancer chemotherapy. *Chinese journal of cancer* vol. 31 51–57 (2012).

76. Gomez-Bougie, P., Halliez, M., Moreau, P., Pellat-Deceunynck, C. & Amiot, M. Repression of Mcl-1 and disruption of the Mcl-1/Bak interaction in myeloma cells couple ER stress to mitochondrial apoptosis. *Cancer Lett.* **383**, 204–211 (2016).

77. Knight, D. W. Feverfew: Chemistry and Biological Activity. *Nat. Prod. Rep.* **12 (3)**, 271 (1995).

78. Sztiller-Sikorska, M. & Czyz, M. Parthenolide as Cooperating Agent for Anti-Cancer Treatment of Various Malignancies. *Pharmaceuticals* vol. 13 (2020).

79. Ghantous, A., Sinjab, A., Herceg, Z. & Darwiche, N. Parthenolide: From plant shoots to cancer roots. *Drug Discov. Today* **18**, 894–905 (2013).

80. Wiedhopf, R. M., Young, M., Bianchi, E. & Cole, J. R. Tumor inhibitory agent from Magnolia grandiflora (Magnoliaceae). I. Parthenolide. *J. Pharm. Sci.* **62**, 345 (1973).

81. Bork, P. M., Schmitz, M. L., Kuhnt, M., Escher, C. & Heinrich, M. Sesquiterpene lactone containing Mexican Indian medicinal plants and pure sesquiterpene lactones as potent inhibitors of transcription factor NF-kappaB. *FEBS Lett.* **402**, 85–90 (1997).

82. Zhang, S., Won, Y.-K., Ong, C.-N. & Shen, H.-M. Anti-cancer potential of sesquiterpene lactones: bioactivity and molecular mechanisms. *Curr. Med. Chem. Anticancer. Agents* **5**, 239–249 (2005).

83. Siedle, B. *et al.* Quantitative structure-activity relationship of sesquiterpene lactones as inhibitors of the transcription factor NF-kappaB. *J. Med. Chem.* **47**, 6042–6054 (2004).

84. Freund, R. R. A., Gobrecht, P., Fischer, D. & Arndt, H. D. Advances in chemistry and bioactivity of parthenolide. *Nat. Prod. Rep.* **37**, 541–565 (2020).

85. García-Piñeres, A. J. *et al.* Cysteine 38 in p65/NF-kappaB plays a crucial role in DNA binding inhibition by sesquiterpene lactones. *J. Biol. Chem.* **276**, 39713–39720 (2001).

86. Kwok, B. H., Koh, B., Ndubuisi, M. I., Elofsson, M. & Crews, C. M. The anti-inflammatory natural product parthenolide from the medicinal herb Feverfew directly binds to and inhibits IkappaB kinase. *Chem. Biol.* **8**, 759–766 (2001).

87. Mathema, V. B., Koh, Y.-S., Thakuri, B. C. & Sillanpää, M. Parthenolide, a sesquiterpene lactone, expresses multiple anti-cancer and anti-inflammatory activities. *Inflammation* **35**, 560–565 (2012).

88. Yang, P.-L., Liu, L.-X., Li, E.-M. & Xu, L.-Y. STAT3, the Challenge for Chemotherapeutic and Radiotherapeutic Efficacy. *Cancers (Basel).* **12**, (2020).

89. Liu, M. *et al.* Parthenolide Inhibits STAT3 Signaling by Covalently Targeting Janus Kinases. *Molecules* vol. 23 (2018).

90. Orofino Kreuger, M. R., Grootjans, S., Biavatti, M. W., Vandenabeele, P. & D'Herde, K. Sesquiterpene lactones as drugs with multiple targets in cancer treatment: focus on parthenolide. *Anticancer. Drugs* **23**, (2012).

91. Liu, Z. *et al.* Modulation of DNA methylation by a sesquiterpene lactone parthenolide. *J. Pharmacol. Exp. Ther.* **329**, 505–514 (2009).

92. Gopal, Y. N. V., Arora, T. S. & Van Dyke, M. W. Parthenolide specifically depletes histone deacetylase 1 protein and induces cell death through ataxia telangiectasia mutated. *Chem. Biol.* **14**, 813–823 (2007).

93. Gazdar, A. F., Oie, H. K., Kirsch, I. R. & Hollis, G. F. Establishment and characterization of a human plasma cell myeloma culture having a rearranged cellular myc proto-oncogene. *Blood* **67**, 1542–1549 (1986).

94. Strober, W. Trypan Blue Exclusion Test of Cell Viability. 3–5 (2015) doi:10.1002/0471142735.ima03bs111.

95. Piccinini, F., Tesei, A., Arienti, C. & Bevilacqua, A. Cell Counting and Viability Assessment of 2D and 3D Cell Cultures : Expected Reliability of the Trypan Blue Assay. 1–12 (2017) doi:10.1186/s12575-017-0056-3.

96. O'Brien, J., Wilson, I., Orton, T. & Pognan, F. Investigation of the Alamar Blue (resazurin) fluorescent dye for the assessment of mammalian cell cytotoxicity. *Eur. J. Biochem.* **267**, 5421–5426 (2000).

97. Munshi, S., Twining, R. C. & Dahl, R. Alamar blue reagent interacts with cell-culture media giving different fluorescence over time: potential for false positives. *J. Pharmacol. Toxicol. Methods* **70**, 195–198 (2014).

98. Präbst, K., Engelhardt, H., Ringgeler, S. & Hübner, H. Basic Colorimetric Proliferation Assays: MTT, WST, and Resazurin BT - Cell Viability Assays: Methods and Protocols. in (eds. Gilbert, D. F. & Friedrich, O.) 1–17 (Springer New York, 2017). doi:10.1007/978-1-4939-6960-9_1.

99. Adan, A., Alizada, G., Kiraz, Y., Baran, Y. & Nalbant, A. Flow cytometry: basic principles and applications. *Crit. Rev. Biotechnol.* **37**, 163–176 (2017).

100. D'Arcy, M. S. Cell death: a review of the major forms of apoptosis, necrosis and autophagy. *Cell Biol. Int.* **43**, 582–592 (2019).

101. Elmore, S. Apoptosis: A Review of Programmed Cell Death. *Toxicol. Pathol.* **35**, 495–516 (2007).

102. Kurosaka, K., Takahashi, M., Watanabe, N. & Kobayashi, Y. Silent cleanup of very early apoptotic cells by macrophages. *J. Immunol.* **171**, 4672–4679 (2003).

103. Lecoeur, H., Ledru, E., Prévost, M. C. & Gougeon, M. L. Strategies for phenotyping apoptotic peripheral human lymphocytes comparing ISNT, annexin-V and 7-AAD cytofluorometric staining methods. *J. Immunol. Methods* **209**, 111–123 (1997).

104. Piaton, E. *et al.* Guidelines for May-Grünwald-Giemsa staining in haematology and non-gynaecological cytopathology: recommendations of the French Society of Clinical Cytology (SFCC) and of the French Association for Quality Assurance in Anatomic and Cytologic Pathology (AFA. *Cytopathology* **27**, 359–368 (2016).

105. Ziegler, U. & Groscurth, P. Morphological Features of Cell Death. *Physiology* **19**, 124–128 (2004).

106. Green, D. R. & Reed, J. C. Mitochondria and apoptosis. *Science* **281**, 1309–1312 (1998).

107. Zorova, L. *et al.* Mitochondrial membrane potential. *Anal. Biochem.* **552**, (2017).

108. Sivandzade, F., Bhalerao, A. & Cucullo, L. Analysis of the Mitochondrial Membrane Potential Using the Cationic JC-1 Dye as a Sensitive Fluorescent Probe. *BIO-PROTOCOL* **9**, (2019).

109. Hsieh, C.-Y. *et al.* Detection of Reactive Oxygen Species During the Cell Cycle Under Normal Culture Conditions Using a Modified Fixed-Sample Staining Method. *J. Immunoass. Immunochem.* **36**, 149–161 (2015).

110. Darzynkiewicz, Z., Juan, G. & Bedner, E. Determining Cell Cycle Stages by Flow Cytometry. *Curr. Protoc. Cell Biol.* **1**, 8.4.1-8.4.18 (1999).

111. Cirera, S. Highly efficient method for isolation of total RNA from adipose tissue. *BMC Res. Notes* **6**, 472 (2013).

112. Wilfinger, W. W., Mackey, K. & Chomczynski, P. Effect of pH and Ionic Strength on the Spectrophotometric Assessment of Nucleic Acid Purity. *Biotechniques* **22**, 474–481 (1997).

113. Mathieson, W. & Thomas, G. A. Simultaneously extracting DNA, RNA, and protein using kits: Is sample quantity or quality prejudiced? *Anal. Biochem.* **433**, 10–18 (2013).

114. Kuang, J., Yan, X., Genders, A. J., Granata, C. & Bishop, D. J. An overview of technical considerations when using quantitative real-time PCR analysis of gene expression in human exercise research. *PLoS One* **13**, e0196438 (2018).

115. Carter, M. & Shieh, J. Molecular Cloning and Recombinant DNA Technology. *Guid. to Res. Tech. Neurosci.* 219–237 (2015) doi:10.1016/b978-0-12-800511-8.00010-1.

116. Svec, D., Tichopad, A., Novosadova, V., Pfaffl, M. W. & Kubista, M. Biomolecular Detection and Quantification How good is a PCR efficiency estimate : Recommendations for precise and robust qPCR efficiency assessments. *Biomol. Detect. Quantif.* **3**, 9–16 (2015).

117. Chesi, M. *et al.* AID-dependent activation of a MYC transgene induces multiple myeloma in a conditional mouse model of post-germinal center malignancies. *Cancer Cell* **13**, 167–180 (2008).

118. Vallabhapurapu, S. & Karin, M. Regulation and function of NF-kappaB transcription factors in the immune system. *Annu. Rev. Immunol.* **27**, 693–733 (2009).

119. Gottesman, M. M., Fojo, T. & Bates, S. E. Multidrug resistance in cancer: role of ATP–dependent transporters. *Nat. Rev. Cancer* **2**, 48–58 (2002).

120. Roque, D. J. C. Mecanismos moleculares associados à resistência adquirida a inibidores do proteasoma em mieloma múltiplo. (Universidade de Coimbra,

2020).

121. Suvannasankha, A. *et al.* Antimyeloma Effects of a Sesquiterpene Lactone Parthenolide. *Clin. Cancer Res.* **14**, 1814–1822 (2008).

122. Wang, W. *et al.* Parthenolide-induced apoptosis in multiple myeloma cells involves reactive oxygen species generation and cell sensitivity depends on catalase activity. *Apoptosis* **11**, 2225–2235 (2006).

123. Pajak, B., Gajkowska, B. & Orzechowski, A. Molecular basis of parthenolide-dependent proapoptotic activity in cancer cells. *Folia Histochem. Cytobiol.* **46**, 129–135 (2008).

124. Cheng, G. & Xie, L. Parthenolide Induces Apoptosis and Cell Cycle Arrest of Human 5637 Bladder Cancer Cells In Vitro. *Molecules* vol. 16 (2011).

125. D'Anneo, A. *et al.* Parthenolide generates reactive oxygen species and autophagy in MDA-MB231 cells. A soluble parthenolide analogue inhibits tumour growth and metastasis in a xenograft model of breast cancer. *Cell Death Dis.* **4**, e891–e891 (2013).

126. Li, H., Lu, H., Lv, M., Wang, Q. & Sun, Y. Parthenolide facilitates apoptosis and reverses drug-resistance of human gastric carcinoma cells by inhibiting the STAT3 signaling pathway. *Oncol Lett* **15**, 3572–3579 (2018).

127. Zhao, X., Liu, X. & Su, L. Parthenolide induces apoptosis via TNFRSF10B and PMAIP1 pathways in human lung cancer cells. *J. Exp. Clin. Cancer Res.* **33**, 3 (2014).

128. Al-Fatlawi, A. A., Al-Fatlawi, A. A., Irshad, M., Rahisuddin & Ahmad, A. Effect of parthenolide on growth and apoptosis regulatory genes of human cancer cell lines. *Pharm. Biol.* **53**, 104–109 (2015).

129. Czyz, M., Lesiak-Mieczkowska, K., Koprowska, K., Szulawska-Mroczek, A. & Wozniak, M. Cell context-dependent activities of parthenolide in primary and metastatic melanoma cells. *Br. J. Pharmacol.* **160**, 1144–1157 (2010).

130. Flores-Lopez, G. *et al.* Parthenolide and DMAPT induce cell death in primitive CML cells through reactive oxygen species. *J. Cell. Mol. Med.* **22**, 4899–4912 (2018).

131. Tang, T.-K., Chiu, S.-C., Lin, C.-W., Su, M.-J. & Liao, M.-H. Induction of survivin inhibition, G_2/M cell cycle arrest and autophagic on cell death in human malignant glioblastoma cells. *Chin. J. Physiol.* **58**, 95–103 (2015).

132. Xiong, S., Chng, W.-J. & Zhou, J. Crosstalk between endoplasmic reticulum stress and oxidative stress: a dynamic duo in multiple myeloma. *Cell. Mol. Life Sci.* **78**, 3883–3906 (2021).

133. Nakaya, A. *et al.* The gold compound auranofin induces apoptosis of human multiple myeloma cells through both down-regulation of STAT3 and inhibition of NF-κB activity. *Leuk. Res.* **35**, 243–249 (2011).

134. Obeng, E. A. *et al.* Proteasome inhibitors induce a terminal unfolded protein response in multiple myeloma cells. *Blood* **107**, 4907–4916 (2006).

135. Lipchick, B. C., Fink, E. E. & Nikiforov, M. A. Oxidative stress and proteasome inhibitors in multiple myeloma. *Pharmacol. Res.* **105**, 210–215 (2016).

136. Santos, C. X. C., Tanaka, L. Y., Wosniak, J. & Laurindo, F. R. M. Mechanisms and implications of reactive oxygen species generation during the unfolded protein response: roles of endoplasmic reticulum oxidoreductases, mitochondrial electron transport, and NADPH oxidase. *Antioxid. Redox Signal.* **11**, 2409–2427 (2009).

137. Cadenas, E. & Davies, K. J. Mitochondrial free radical generation, oxidative stress, and aging. *Free Radic. Biol. Med.* **29**, 222–230 (2000).

138. Hempel, N. & Trebak, M. Crosstalk between calcium and reactive oxygen species signaling in cancer. *Cell Calcium* **63**, 70–96 (2017).

139. Yan, Y., Wei, C., Zhang, W., Cheng, H. & Liu, J. Cross-talk between calcium and reactive oxygen species signaling. *Acta Pharmacol. Sin.* **27**, 821–826 (2006).

140. Gao, H.-E. *et al.* Antineoplastic effects of CPPTL via the ROS/JNK pathway in acute myeloid leukemia. *Oncotarget* **8**, 38990–39000 (2017).

141. Sun, J. *et al.* Parthenolide-induced apoptosis, autophagy and suppression of proliferation in HepG2 cells. *Asian Pac. J. Cancer Prev.* **15**, 4897–4902 (2014).

142. Kwak, S. W., Park, E. S. & Lee, C. S. Parthenolide induces apoptosis by activating the mitochondrial and death receptor pathways and inhibits FAK-mediated cell invasion. *Mol. Cell. Biochem.* **385**, 133–144 (2014).

143. Ichim, G. & Tait, S. W. G. A fate worse than death: apoptosis as an oncogenic process. *Nat. Rev. Cancer* **16**, 539–548 (2016).

144. Anguiano, A. *et al.* Gene expression profiles of tumor biology provide a novel approach to prognosis and may guide the selection of therapeutic targets in multiple myeloma. *J. Clin. Oncol.* **27**, 4197–4203 (2009).

145. Lin, M. *et al.* Parthenolide suppresses non-small cell lung cancer GLC-82 cells growth via B-Raf/MAPK/Erk pathway. *Oncotarget* **8**, 23436–23447 (2017).

146. Bretones, G., Delgado, M. D. & León, J. Myc and cell cycle control. *Biochim. Biophys. Acta* **1849**, 506–516 (2015).

147. Oeckinghaus, A. & Ghosh, S. The NF-kappaB family of transcription factors and its regulation. *Cold Spring Harb. Perspect. Biol.* **1**, a000034 (2009).

148. Kitada, S., Pedersen, I. M., Schimmer, A. D. & Reed, J. C. Dysregulation of apoptosis genes in hematopoietic malignancies. *Oncogene* **21**, 3459–3474 (2002).

149. Liu, J.-W. *et al.* Parthenolide induces proliferation inhibition and apoptosis of pancreatic cancer cells in vitro. *J. Exp. Clin. Cancer Res.* **29**, 108 (2010).

150. Naseri, M. H. *et al.* Up regulation of Bax and down regulation of Bcl2 during 3-NC mediated apoptosis in human cancer cells. *Cancer Cell Int.* **15**, 55 (2015).

151. Kim, I. H. *et al.* Parthenolide-induced apoptosis of hepatic stellate cells and anti-fibrotic effects in an in vivo rat model. *Exp. Mol. Med.* **44**, 448–456 (2012).